Holograms of speckle fields

B. Ya. Zel'dovich, V. V. Shkunov, and T. V. Yakovleva

Institute of Problems in Mechanics, Academy of Sciences of the USSR, Moscow
Usp. Fiz. Nauk **149**, 511–549 (July 1986)

Studies on the electrodynamic theory of the process of readout of holograms recorded in the interference of an object speckle field and a smooth reference wave are reviewed. These holograms are classified as thin, thick-layer, and volume holograms, and the process of reconstitution is examined from a unitary standpoint for all these types of holograms. Calculations are performed of the diffraction efficiency and noise level with account taken of various physical factors: saturation of the photoresponse, shift in frequency and angle during reconstruction, shrinkage of the hologram material, etc. Substantial advantages of volume holograms are demonstrated with respect to efficiency and quality of reconstruction in the next five years and in the prospects up to the year 2000.

TABLE OF CONTENTS

1. INTRODUCTION

The statement that holography is widely applied for scientific and imaging purposes has long since become a truism. Holographic interferometry for remote monitoring of strains, stresses, and displacements of solid bodies; the recording, storage, and parallel optical processing of large masses of information; holographic Fresnel lenses and other optical elements of low thickness and mass for the visible and infrared ranges; holographic displays for training apparatus; imaging holography and holographic cinema with the complete illusion of a solid object—this is far from being a complete list of the fields of application of the methods of holography.[1–6] In almost all applications of holography the important parameters are: 1) the efficiency of reconstruction by the hologram of the exact field of the object; 2) the quality of reconstruction, as characterized by the ratio of the intensities of the signal and the distortions. To determine and optimize these parameters, one needs a detailed quantitative understanding of the electrodynamic processes that occur in the recording medium in reccording and readout of holograms.

As N. Bloembergen[76] has noted, "in a certain sense one can also include holography among the nonlinear optical phenomena." Hence it is not fortuitous that the mathematical methods of solving electrodynamic problems of nonlinear optics, and in particular, the method of truncated equations, so fruitfully developed by R. V. Khokhlov[1),23,77,78] have substantially aided advances in solving the electrodynamic problems of holography.

In the early studies on holography,[7–9] the fundamental aim was to prove the mere fact of reconstruction of a wave front. Hence the complex electrodynamic process of conversion of the reconstructing reference wave into the object field was replaced by the following simple considerations, albeit

 0038-5670/86/070678-25$01.80

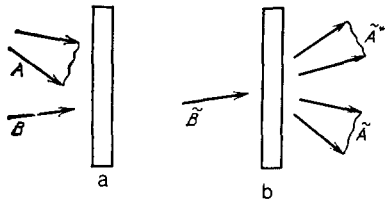

FIG. 1. Diagrams of the recording of a hologram with an object field A and a reference field B (a) and of reconstruction of the field $\tilde{A}$ using the reference wave $\tilde{B}$ (b).

sufficient to this purpose. Let the field being recorded with the complex amplitude $E(\mathbf{r}) = A(\mathbf{r}) + B(\mathbf{r})$ consist of two mutually coherent components: the reference wave $B(\mathbf{r})$ and the object wave $A(\mathbf{r})$, and let it record in the medium perturbations proportional to the local intensity $|E(\mathbf{r})|^2 = (A + B)(A^* + B^*)$ (Fig. 1). Further, one assumes that in the reconstruction with the same reference field $\tilde{B}(\mathbf{r}) = B$ the hologram operates as a transparency having a coefficient of amplitude transmission $t(\mathbf{r})$ connected linearly with the intensity in recording: $t(\mathbf{r}) - t_0 = t_1|E(\mathbf{r})|^2$. If we consider in $t(\mathbf{r})$ only the reference terms $A(\mathbf{r})B^*(\mathbf{r}) + A^*(\mathbf{r})B(\mathbf{r})$, we obtain the following expression for the reconstructed field:

$$E_{\text{recon}}(\mathbf{r}) = t_1 A(\mathbf{r})\,|B|^2 + t_1 A^*(\mathbf{r})\,B^2. \qquad (1.1)$$

Thus the complex field of the object wave $\tilde{A}(\mathbf{r}) \propto A(\mathbf{r})$ is reconstructed at the output of the hologram.

In view of the well-known Huygens principle, this wave in the space beyond the hologram is indistinguishable from the field in recording, which bears a volume image of the object. In a direction approximately symmetric with respect to the reference wave, the hologram reconstructs the so-called pseudoscopic, or real image, which corresponds to the complex conjugate wave $\tilde{A}(\mathbf{r}) \propto A^*(\mathbf{r})$.

In a simple treatment by Eq. (1.1), the possible distortions (noise) in the reconstructed wave were omitted from the very outset. Moreover, the linear dependence $t - t_0 = t_1|E(\mathbf{r})|^2$ is known to break down in the very interesting case in which we wish to obtain a hologram with a high diffraction efficiency of reconstruction of the object field. Finally, for photolayers of appreciable thickness L (under typical conditions with $L > 10^{-3}$ cm), the diffraction of the field is substantial already inside the hologram,[10] and its action on the incident field cannot be described in terms of a transparency with a given transmission. Therefore, to determine the diffraction efficiency of the hologram and the magnitude of the distortions in the general case requires solving the electrodynamic problem in its full scope.

In the model situation in which both the reference (B) and object (A) waves are considered plane waves with constant amplitude, this problem was already solved at the dawn of laser holography[11,12] by methods previously developed in the theory of diffraction of light by ultrasonic waves and in the theory of x-ray diffraction in crystals. The possibility of transferring these methods into holography involved the assumption of exact regularity of the sinusoidal holographic grating.

However, in the overwhelming number of cases the local behavior of the field of the object wave $A(\mathbf{r})$ is extremely irregular and does not at all resemble the object itself. In fact, the field $A(\mathbf{r})$ at a given point $\mathbf{r}$ of the hologram is the result of coherent superposition of the contributions from different illuminated points of the object. For objects of arbitrarily complex shape, these contributions have random phases that differ at different points of the hologram. Owing to interference the field $A(\mathbf{r})$ in the plane of the hologram has the so-called speckle structure (Fig. 2), i.e., marked random spatial inhomogeneities of intensity and phase (see Refs. 13–15 on speckle fields). In contrast to this, the mean statistical characteristics of the field $A(\mathbf{r})$ in the plane of the hologram, and in particular, the mean intensity $\langle |A(\mathbf{r})|^2 \rangle$ proves to be practically homogeneous throughout the cross-section, even for an object with an evidently inhomogeneous brightness, e.g., for a bright object on a black background far from the hologram.

Only in recent years has a sufficiently complete theory of holograms of speckle fields been created, combining the electrodynamics of diffraction and the statistics of speckle inhomogeneities, and the first experimental confirmations of this theory have appeared. This review is devoted, in accord with its title, to precisely these problems.

In the literature one sometimes meets the term "hologram of a diffuse object," which presupposes the presence of speckle structure in the field directly at the object. The concept of the "hologram of a speckle field" is broader, since the speckle structure of the object field in the plane of the photofilm is formed even for objects not diffuse in nature, such as an information transparency, a slide with text, and even a specular object of complex shape.

2. CLASSIFICATION OF HOLOGRAMS OF SPECKLE FIELDS

2.1. Speckle fields

We are convinced that every reader of this review has seen a speckle field. Speckle structure arises when a diffusely reflecting surface, e.g., the walls of a room or the pages of a book, is illuminated with coherent laser light. This term arises from the English "speckle"—a speck or spot on the skin. The region of the surface illuminated by the laser seems

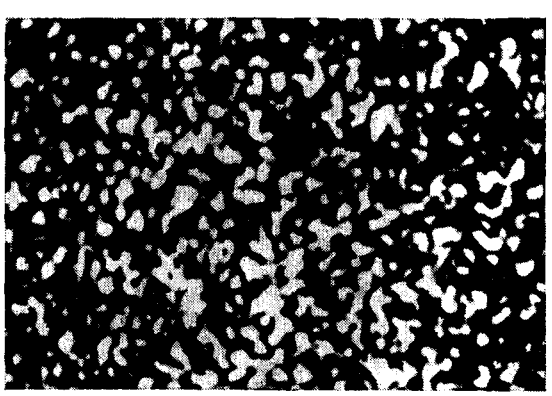

FIG. 2. Enlarged photograph of a region of the transverse section of a speckle field.

to sparkle. That is, it consists of very tiny spots (of dimension usually determined by the limit of resolution of the eye) that make a fanciful display as the observer, the scatterer, or the laser source moves. Actually, the coherent light wave reflected by the object creates an intensity distribution in space with a very large number of fine-structure inhomogeneities. In this section we shall discuss the statistical characteristics of this distribution, as well as its characteristic spatial scales.

As we have already noted in the Introduction, the complex amplitude of the field at every given point is composed of a large number of small independent contributions, namely the waves reflected by different points of the object. In this situation the central limit theorem of probability theory can be applied to the resulting field. According to it the amplitude of the total field will have a random nature in space and will be described by Gaussian statistics.

While referring to the textbooks on probability theory, statistical radiophysics, and optics[15,20–22] for the details of derivation of this theorem, we shall formulate a set of consequences for the properties of the random complex amplitude $A(\mathbf{R})$ of the speckle field, where $\mathbf{R}$ is the space-coordinate vector.

The probability distribution for the complex amplitude of the speckle field at a given point has a Gaussian form:

$$\begin{aligned} &dP = W(A)\, d\,\mathrm{Re}\,A\, d\,\mathrm{Im}\,A, \\ &W = \frac{1}{\pi I_A}\exp\left[-\frac{(\mathrm{Re}\,A)^2}{I_A} - \frac{(\mathrm{Im}\,A)^2}{I_A}\right]. \end{aligned} \tag{2.1}$$

Hence the amplitude of the field at the given point has the Rayleigh distribution

$$dP = \frac{2}{I_A}|A|\exp\left(\frac{-|A|^2}{I_A}\right) d|A|, \tag{2.2}$$

while the phase $\varphi = \tan^{-1}(\mathrm{Im}\,A/\mathrm{Re}\,A)$ is uniformly distributed in the interval from 0 to 2. Finally, the probability distribution for the local intensity $I(\mathbf{R}) = |A(\mathbf{R})|^2$ has the exponential form

$$dP = I_A^{-1}\exp\left(-\frac{I}{I_A}\right) dI. \tag{2.3}$$

In Eqs. (2.1)–(2.3) I_A denotes the mean intensity: $I_A = \langle I\rangle$.

The Gaussian character of the statistics of the speckle field has important consequences. Thus Eqs. (2.1)–(2.3) imply that

$$\langle I^2\rangle = 2\langle I\rangle^2 = 2I_A^2, \quad \langle (I - I_A)^2\rangle = I_A^2. \tag{2.4}$$

The angle brackets denote averaging over the probability distribution of (2.3); for statistically homogeneous fields we have $I_A(\mathbf{R}) = \text{const}$, and this is equivalent to averaging over space. According to (2.4) the relative depth of modulation of the intensity, i.e., the contrast of the speckle structure, amounts to a quantity of the order of unity. The transverse and longitudinal dimensions of the inhomogeneities are determined by the angle of convergence of the elementary interfering waves of which the speckle field consists. Mathematically this is expresseed in the fact that the spatial correlation function $\gamma(\mathbf{R}_1 - \mathbf{R}_2)$ of the random monochromatic field $A(\mathbf{R})e^{-i\omega t}$ is connected[15,18,20–22] to the angular spectrum $j(\theta)$ by the Van Cittert-Zernike theorem:

$$\begin{aligned} \gamma(\mathbf{R}) &= \frac{\langle A^*(\mathbf{R}_1)\, A(\mathbf{R}_1+\mathbf{R})\rangle}{\langle |A|^2\rangle} \\ &= e^{ikz}\int d^2\theta\, j(\theta)\exp\left[ik\left(\mathbf{r}\theta - \frac{1}{2}z\theta^2\right)\right]. \end{aligned} \tag{2.5}$$

In Eq. (2.5) we have distinguished the central direction of propagation of the speckle field (the z axis) so that $\mathbf{R} = \mathbf{r} + z\mathbf{e}_z$; $\mathbf{r}$ is the coordinate in the transverse plane, $\mathbf{r} = \mathbf{e}_x x + \mathbf{e}_y y$, the angles $\theta = \mathbf{e}_x\theta_x + \mathbf{e}_y\theta_y$ are assumed to be not too large, $|\theta| \lesssim 1$, and $k = \omega n/c$, where n is the refractive index.

The transverse dimension of the inhomogeneity of a speckle field can be estimated from the uncertainty relationship: $|\Delta\mathbf{r}| \sim \lambda/|\Delta\theta|$, where $|\Delta\theta|$ is the width of the angular spectrum. A field with the transverse inhomogeneity $|\Delta\mathbf{r}|$ and the divergence $|\Delta\theta|$ appreciably alters the intensity profile at a mixing distance of the rays of $\Delta z \approx |\Delta\mathbf{r}|/|\Delta\theta| \sim \lambda/|\Delta\theta|^2$. These same estimates can be easily derived also from Eq. (2.5). Thus, for radiation having a spectrum of the form $j(\theta) \propto \exp(-\theta^2/\theta_0^2)$ the correlation function $\gamma(\mathbf{R})$ has the form:

$$\gamma(\mathbf{R}) = \frac{1}{1+i\alpha^2}\exp\left(ikz - \frac{1}{4}\frac{k^2\mathbf{r}^2\theta_0^2}{1+i\alpha}\right), \quad \alpha = \frac{kz\theta_0^2}{2}. \tag{2.6}$$

We shall define the characteristic scales of the inhomogeneities in $\mathbf{r}$ and in z by the condition that the quantity $|\gamma|^2$ should decrease to a certain definite value:

$$\Delta r\,(\mathrm{HW}e^{-1}\mathrm{M}) = \frac{\lambda}{\pi\sqrt{2}\,\theta_0}, \quad \Delta z\left(\mathrm{HW}\,\frac{1}{2}\,\mathrm{M}\right) = \frac{\lambda}{\pi\theta_0^2}, \tag{2.7}$$

Here λ and θ are the wavelength and the angle, both being defined in the medium; $\mathrm{HW}e^{-1}\mathrm{M}$ denotes the half-width at the level of e^{-1} of the value at the maximum (Half-Width e^{-1} Maximum).

A remarkable property of random fields having Gaussian statistics is that a knowledge of the correlation function for the field A [i.e., $\gamma(\mathbf{R})$] enables one to find any of the higher correlators. In particular, the intensity $I(\mathbf{R})$ obeys the equation

$$\langle I(\mathbf{R}_1)\, I(\mathbf{R}_1 + \mathbf{R})\rangle = \langle I\rangle^2[1 + |\gamma(\mathbf{R})|^2], \tag{2.8}$$

We see from this that the longitudinal and transverse scales of the intensity correlations are the same as for the correlation of the field itself.

2.2. Types of holograms

Let the exposure of the hologram to the overall field of the reference wave $Be^{i\mathbf{k}_B\cdot\mathbf{R}}$, and the object wave $A(\mathbf{R})\,e^{i\mathbf{k}_A\cdot\mathbf{R}}$, and the subsequent processing result in acquisition by the hologram of a dielectric permittivity that depends on the spatial coordinates $\mathbf{R} \equiv (\mathbf{r}, z) \equiv (x, y, z)$ according to the law

$$\begin{aligned} \varepsilon(\mathbf{R}) = \bar{\varepsilon} &+ \beta_1(|B|^2 + |A|^2) \\ &+ \beta_2\{A(\mathbf{R})\, B^*\exp[i(\mathbf{k}_A - \mathbf{k}_B)\mathbf{R}] \\ &+ A^*(\mathbf{R})\, B\exp[-i(\mathbf{k}_A - \mathbf{k}_B)\mathbf{R}]\}. \end{aligned} \tag{2.9}$$

Here we shall employ an expression of the following type to represent the real monochromatic waves:

$$E(\mathbf{R}, t) = \frac{1}{2}[E(\mathbf{R})e^{-i\omega t} + E^*(\mathbf{R})e^{i\omega t}].$$

A modulation of the type of (2.9) leads to a change in the local refractive index:

$$n(\mathbf{R}) = n_0 + \frac{\beta_1(|B|^2 + |A|^2)}{2n_0} + \Delta n_{AB}\cos[(\mathbf{k}_A - \mathbf{k}_B)\mathbf{R} + \varphi_A - \varphi_B],$$

$$\Delta n_{AB} = \beta_2 |AB^*| n_0^{-1}. \quad (2.10)$$

Here $\mathbf{k}_A$ and $\mathbf{k}_B$ are the wave vectors for the central directions of the waves A and B during recording, $A(\mathbf{R})$ is the slowly varying amplitude of the object wave, $B = \text{const}$ is the amplitude of the plane reference wave, Δn_{AB} is the amplitude (span to one side) of the lattice. The coefficient β_1 characterizes the response of the medium to illumination with a smooth spatial distribution, i.e., to illumination with intensities of both waves A and B without allowance for their mutual interference. Since these inhomogeneities are caused by the coherent superposition of the components inside the angular spectrum of the object wave, they are called *intramodulational*.[2)]

The holographic grating proper arises from the interference between the fields A and B during recording, and the contribution to $\varepsilon(\mathbf{R})$, which is proportional to β_2 in Eq. (2.9), is called *cross-modulational*. The cross grating has the rather small spatial period $\Lambda = 2\pi/|\mathbf{k}_A - \mathbf{k}_B| = \lambda / 2\sin(\theta_{AB}/2)$.

In most cases the finite spatial resolution of the photomaterial causes the response $|\beta_2|$ of the medium at high spatial frequencies to be weaker than at low frequencies: $|\beta_2| < |\beta_1|$.[3)] Moreover, the incomplete coherence of the reference and object waves also diminishes the coefficient β_2. The positive imaginary component of the coefficients β_1 and β_2 corresponds to absorption of the waves in the process of reconstruction caused by the exposure during recording. Negative $\operatorname{Im}\beta_1$ and $\operatorname{Im}\beta_2$ correspond to media in which the former, initially homogeneous absorption is saturated by the exposure, and also to media with light-induced amplification.

The methods of solution of the electrodynamic problem of reconstruction of the object field by the hologram prove to differ for the so-called thin, thick-layer, and volume (or three-dimensional) holograms. The classification of holograms according to the types cited above is determined by the relationship between the thickness of the photolayer and the spatial scales characterizing the diffraction of the light fields. In this connection we shall discuss the scales of the inhomogeneities recorded in the medium (Fig. 3).

Let us denote the transverse scale of the inhomogeneity of the field as a. Then by the uncertainty relationship it corresponds to the angular divergence $\Delta\theta \sim \lambda/a$, where λ is the wavelength of the light. The light rays at the distance $l_{\text{Fr}} \sim a/\Delta\theta \approx \lambda/(\Delta\theta)^2$, which is called the Fresnel length, extend beyond the limits of the original inhomogeneity. At distances $z \lesssim l_{\text{Fr}}$ the simple laws of geometric optics are applicable, while when $z \gg l_{\text{Fr}}$, diffraction processes become substantial.

For the cross-grating that is recorded by the interference of the fields A and B converging at the angle θ_{AB} to one another (Fig. 3), the dimension a corresponds to the period $\Lambda \approx \lambda/\theta_{AB}$. If the thickness L of the photofilm is smaller than the Fresnel length of the cross-grating (i.e., if $L < \lambda/\theta_{AB}^2$), then the diffraction inside the layer is inessential, and the hologram behaves like a transparency:

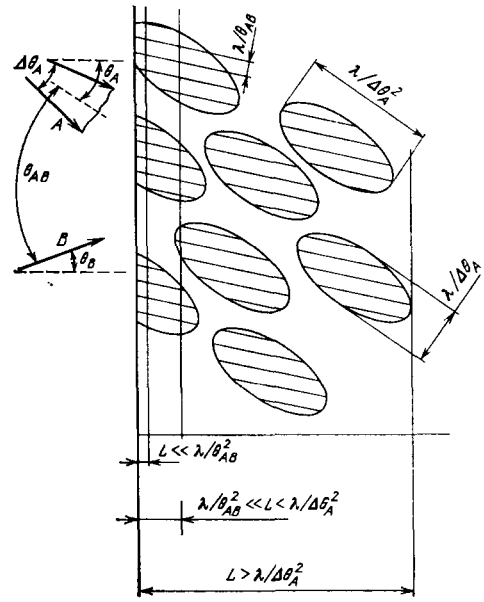

FIG. 3. Scales of the interference inhomogeneities in holograms of different types: thin, thick-layer, and volume.

$$E_{\text{trans}}(\mathbf{r}) = E_{\text{incid}}(\mathbf{r})\, t(\mathbf{r}). \quad (2.11)$$

Here $t(\mathbf{r})$ is determined by the local value of $\varepsilon(\mathbf{r})$ at the given point of the hologram. Under these same conditions $\varepsilon(\mathbf{R})$ does not depend on the coordinate z normal to the photolayer. Such holograms are called *thin*. Only for thin holograms does the qualitative description in the form (1.1) hold. Precisely for them do two images simultaneously arise—an imaginary one (the object field $A(\mathbf{r})$) and a real pseudoscopic one ($A^*(\mathbf{r})$), and with about the same efficiency (see Fig. 1b). If the nonlinear terms in the dependence of $t(\mathbf{r})$ on the intensity of the interference recording pattern are also substantial, then higher orders of diffraction also arise in thin holograms.

For a field $A(\mathbf{R})$ having a complex spatial structure, the amplitude and phase of the holographic grating $A(\mathbf{R})B^*$ depend smoothly on the coordinates (on the scale of its period). The characteristic transverse scale $a_1 \sim \lambda/\Delta\theta_A$ of the inhomogeneity of the field $A(\mathbf{R})$ is determined by the angular width $\Delta\theta_A$ of the object wave, i.e., the angle $\Delta\theta_A$ over which the illuminated part of the object is visible from the surface of the hologram. This transverse dimension of the speckle element corresponds to the longitudinal dimension $l_{\text{Fr}} = \lambda/\Delta\theta_A^2$.

If the thickness L of the photofilm obeys the condition $\lambda/\theta_{AB}^2 \ll L \lesssim \lambda/\Delta\theta_A^2$, the hologram is termed a *thick-layer* one.

The condition $\lambda/\theta_{AB}^2 \ll L$ ensures the excitation of

only one object field during reconstruction. The remaining orders of diffraction do not satisfy the Bragg condition and are not excited; in particular this pertains to the conjugate image. On the other hand, the condition $L < \lambda / \Delta\theta_A^2$ enables one to consider the amplitude and phase of the cross-grating to be constant throughout the depth of the hologram and within the limits of an area having the transverse dimension of a speckle spot $\sim \lambda / \Delta\theta_A$. In such a region we can consider both the reference and the object wave to be plane. Thus, in order to solve the electrodynamic problem of field reconstruction by a thick-layer hologram, it suffices to apply locally the theory of interaction of two (only two!) plane waves, despite the fact that the object speckle field itself contains waves in different directions.

Finally, in the case $L \gg \lambda / \Delta\theta_A^2 \gtrsim \lambda / \theta_{AB}^2$, many speckle elements of the object wave are contained within the thickness L of the photolayer (see Fig. 3). Such holograms are called *volume* (or three-dimensional) holograms. The formulation of the electrodynamic problem here proves most complex, since the amplitude and phase of the cross-grating are changed many times in irregular fashion along the path of the ray in the hologram. The study of volume holograms is of pragmatic, as well as purely intellectual, interest; it will be evident below that precisely these holograms possess high diffraction efficiency with a small noise level, which distinguishes them from thin and thick-layer holograms of speckle fields. Strictly speaking, a number of intermediate cases falls outside our classification, such as $L \sim \lambda / \theta_{AB}^2$, the case of a spreading reference wave, etc. However, these cases are rather rarely employed in optical holography of speckle fields.

Up to now we have been describing the so-called transmission holograms, in which the reference and object waves are incident on the photolayer from the same side. The reflection holograms recorded by the system of Yu. N. Denisyuk are widely applied and are of great interest. In them the reference and object waves are incident on the photolayer from different sides, approximately in opposition. In this case the layers of the cross-grating are approximately parallel to the boundaries of the photolayer, while the period of the grating is $\lambda/2$; here λ is the wavelength of the light in the medium. Usually the thickness of the photolayer amounts to no less than several micrometers. Hence reflection holograms are either thick-layer or volume holograms. Formally we can assume in all the previous estimates that $\theta_{AB} \sim 2$ radians for reflecting holograms.

3. AMPLITUDE OF THE RECONSTRUCTED FIELD AND THE DIFFRACTION EFFICIENCY

Before discussing the specific properties introduced by the speckle structure of the object field in the reconstruction process, in Secs. 3 and 4 we shall discuss the diffraction efficiency and the selective properties of holograms recorded by the interference of two plane waves. We shall do this in the first Born approximation of scattering theory, i.e., in the first order of perturbation theory in the amplitude of the cross-grating $\beta_2 B^* A$. In this approximation the stated properties of holograms do not depend on the type of hologram nor on the kind of object wave—plane or having speckle structure—since the amplitude of the reconstructed field $\tilde{A}$ is linearly related to the amplitude A of the field during recording, and the superposition principle holds. Thus the results of Secs. 3 and 4 are equally applicable to holograms with any kind of object field.

We shall adopt the wave equation describing the propagation of the complex amplitude $E(\mathbf{R})e^{-i\omega t}$ in the form of the Helmholtz equation

$$\Delta E + \frac{\omega^2}{c^2}[\varepsilon_0 + \delta\varepsilon(\mathbf{R})]E(\mathbf{R}) = 0. \tag{3.1}$$

Here ω is the frequency of the monochromatic field, $\omega = 2\pi c/\lambda_0$, and c and λ_0 are the speed of light and the wavelength *in vacuo*. In honesty we must warn the reader that Eq. (3.1) in the most general case of arbitrarily polarized fields in a medium with arbitrary inhomogeneities is not valid. The correct vector equation has the form:

$$\operatorname{rot}\operatorname{rot}\mathbf{E} - \left(\frac{\omega}{c}\right)^2[\varepsilon_0 + \delta\varepsilon(\mathbf{R})]\mathbf{E} = 0.$$

However, Eq. (3.1) proves valid for the case, especially important in holography, in which the polarizations of all the interacting waves are the same and we can restrict the treatment to the scalar case.

Let us represent the total field $E(\mathbf{R})$ in the form of an incident reference wave $\tilde{B}e^{i\mathbf{k}_B\cdot\mathbf{R}}$ plus the result of scattering $E_1(\mathbf{R})$. That is, we have $E(\mathbf{R}) = \tilde{B}e^{i\mathbf{k}_B\cdot\mathbf{R}} + E_1(\mathbf{R})$. If we assume that $E_1(\mathbf{R})$ is a quantity of the first order of smallness in $\delta\varepsilon$, we obtain the following from (3.1):

$$\Delta E_1 + k_0^2 E_1(\mathbf{R}) = -k_0^2 \frac{\delta\varepsilon(\mathbf{R})}{\varepsilon_0}\tilde{B}e^{i\mathbf{k}_B\mathbf{R}}. \tag{3.2}$$

Here and below, the symbol $\sim$ will refer to fields in the process of reconstruction. This approximation, which in the quantum-mechanical theory of scattering is commonly called the "Born approximation," is valid if $|E_1| \ll |\tilde{B}|$, i.e., when the efficiency of scattering is small. Remarkably, very many important properties of holograms can be studied even in this approximation.

One can easily write an explicit solution of Eq. (3.2) that satisfies the Sommerfeld radiation principle. However, it is more convenient to discuss the results obtained for each angular component of the scattered field E_1 separately. Therefore we shall assume initially that the object wave during recording is plane, $e^{i\mathbf{k}_A\cdot\mathbf{R}}A(\mathbf{R}) = Ae^{[i\mathbf{k}_A\cdot\mathbf{R}]}$ with $A = \text{const}$. Owing to the linearity of the cross-modulation terms in $\delta\varepsilon$ from (2.9) with respect to $A(\mathbf{R})$ and the linearity of Eq. (3.1), the result for an object wave having a complex angular spectrum is obtained by simple superposition of the results for the individual angular components.

The aim of the electrodynamic problem that we are solving is to find the reconstructed object wave $\tilde{A}$ at the output of the hologram, i.e., in the cross-section $z = L$. To do this, we must leave the cross-modulation term $\delta\varepsilon = \beta_2 B^* A e^{i(\mathbf{k}_A - \mathbf{k}_B)\cdot\mathbf{R}}$, which describes the scattering in the direction of the object, on the right-hand side of Eq. (3.2) inside the photolayer, i.e., for $0 \leqslant z < L$. The term complex conjugate to it is responsible for the formation of the accompanying reference wave of the pseudoscopic image, in

which we shall not be interested. In the same first Born approximation, the reconstructing wave does not vary as it propagates through the hologram, or $B = \text{const}$.

Then the solution for the field $E_1(\mathbf{R})$ can be naturally sought in the form $E_1(\mathbf{R}) = \widetilde{A}(z)e^{i\mathbf{k}_A\cdot\mathbf{R}}$, where $\widetilde{A}(z)$ is the amplitude, which varies slowly on the scale of the wavelength. Then one obtains from (3.2) a truncated equation[23] for $\widetilde{A}(z)$ that yields the following with the boundary condition $\widetilde{A}(z=0) = 0$:

$$2ik\cos\theta_A \frac{d\widetilde{A}}{dz} = -\frac{k^2\beta_2}{\varepsilon_0} B^*\widetilde{B}A, \qquad \widetilde{A}(z=L) = \widetilde{B}\frac{ikL\beta_2 B^*A}{2\varepsilon_0\cos\theta_A}. \tag{3.3}$$

The quantity $L/\cos\theta_A$ is the path length over which the object wave being reconstructed coherently gains its amplitude inside the photolayer. The second relationship of (3.3) enables one to find the diffraction efficiency of the hologram, which is equal to the fraction of the energy of the reference wave scattered into the image (into the field $\widetilde{A}$). In the diffraction of the beam $\widetilde{B}$ into the beam $\widetilde{A}$ in a region of the hologram of area S, the cross section of the reconstructed beam has an area $S_A = S\cos\theta_A$, while the cross section of the reference beam $\widetilde{B}$ has the area $S_B = S|\cos\theta_B|$. Hence the energy ratio of these beams, which yields the diffraction efficiency η, is

$$\eta = |M|^2 = \frac{|\widetilde{A}|^2 S_A}{|\widetilde{B}|^2 S_B} = \left|\frac{\widetilde{A}}{\widetilde{B}}\right|^2 \frac{\cos\theta_A}{|\cos\theta_B|}. \tag{3.4}$$

Here we have introduced the dimensionless characteristic of the strength of the cross-grating $\beta_2 AB^*$ within the thickness L of the hologram:

$$M = \frac{kL\beta_2|AB^*|}{2\varepsilon_0(\cos\theta A\cdot|\cos\theta_B|)^{1/2}} = \frac{\omega}{2c}\Delta n_{AB}\frac{L}{(\cos\theta_A\cdot|\cos\theta_B|)^{1/2}}. \tag{3.5}$$

Henceforth we shall call the quantity M the *strength of the hologram*.

Let us make some very simple estimates. For the radiation of a red-light laser we have $\lambda = 0.63\ \mu\text{m}$, $\omega/c = 2\pi/\lambda = 10^5\ \text{cm}^{-1}$. For a typical thickness of a photolayer $L \simeq 7\ \mu\text{m}$, the strength of the hologram is $|M| = 35\ \Delta n_{AB}$. This estimate shows that the hologram can have a relatively large strength, $|M| \sim 1$, i.e., an appreciable diffraction efficiency, with a rather modest value $\Delta n_{AB} = 0.03$. The reason for this consists in the coherent addition of the diffracted waves from a large number of elementary layers of thickness of the order $\lambda/2\pi$ and is mathematically manifested in the form of a large dimensionless coefficient $2\pi L/\lambda$.

4. SPECTRAL-ANGULAR SELECTIVITY

Thus far we have assumed that the mean refractive index and the thickness of the photolayer were not altered by the processing of the hologram, and that in the reconstruction the hologram is illuminated with a reference wave of exactly the same frequency and direction as in recording. Actually this is not always so. During the chemical processing an effect of shrinkage of the photolayer occurs, its mean refractive index is altered, and the readout wave is often formed by a non-point source of white light, which therefore has an extended angular and frequency spectrum. Owing to the linearity of the wave equation, it suffices at first to solve the problem of reconstruction for a plane monochromatic readout wave $\widetilde{B}\exp(-i\widetilde{\omega}t + i\mathbf{k}_{\widetilde{B}}\cdot\mathbf{R})$, in which, however, the frequency and direction of incidence differ from those during recording. Thereupon the result of reconstruction by a reference wave with extended angular and frequency spectra is given by the superposition of the results for each of the components.

4.1. Form of the selectivity curve

Let $\mathbf{Q}$ be the cross-grating vector in the processed photolayer, i.e.,

$$\varepsilon(\mathbf{R}) = \widetilde{\varepsilon} + \beta_2 AB^*e^{i\mathbf{QR}} + \beta_2 A^*Be^{-i\mathbf{QR}}. \tag{4.1}$$

Then the Helmholtz Equation (3.1) in the first Born approximation is reduced to

$$\Delta E_1 + \widetilde{k}^2 E_1 = -\left(\frac{\widetilde{\omega}}{c}\right)^2 \beta_2 AB^*\widetilde{B}\exp[i(\mathbf{k}_{\widetilde{B}} + \mathbf{Q})\mathbf{R}]. \tag{4.2}$$

The right-hand side in Eq. (4.2) will efficiently excite the reconstructed image $\widetilde{A}$ if the Bragg condition is satisfied for the diffraction of the reconstructing reference wave by the grating from (4.1):

$$(\mathbf{k}_{\widetilde{B}} + \mathbf{Q})^2 = \widetilde{k}^2 \equiv \left(\frac{\widetilde{\omega}}{c}\right)^2 \widetilde{\varepsilon}. \tag{4.3}$$

From the mathematical standpoint (4.3) is the condition that the right-hand side of (4.2) is a solution of the homogeneous equation from the left-hand side of (4.2). Geometrically the Bragg condition (4.3), which is well known from the theory of diffraction of x-rays in crystals, corresponds to the idea that the angle of incidence of the wave $\widetilde{\mathbf{k}}_{\widetilde{B}}$ on the layers of the grating is equal to the angle of reflection, while the phase shift in the reflection of the waves from adjacent layers is 2π.

By traditional methods one can derive from (4.2) the following truncated equation for the slow amplitude $\widetilde{A}(z)$ of the object wave being reconstructed $\widetilde{A}(z)\exp(-i\widetilde{\omega}t + i\mathbf{k}_{\widetilde{A}}\cdot\mathbf{R})$:

$$\frac{d\widetilde{A}(z)}{dz} = De^{i\Delta kz}, \qquad D = \frac{i\widetilde{k}\beta_2 AB^*\widetilde{B}}{2\widetilde{\varepsilon}\cos\widetilde{\theta}_A}, \qquad \Delta k = (\mathbf{k}_{\widetilde{B}} + \mathbf{Q} - \mathbf{k}_{\widetilde{A}})_z. \tag{4.4}$$

Its solution with $\widetilde{A}(z=0) = 0$ is

$$\widetilde{A}(z=L) = D\frac{e^{i\Delta k\cdot L} - 1}{i\Delta k} \equiv De^{iX}\frac{\sin X}{X}, \qquad X = \frac{\Delta k\cdot L}{2} \tag{4.5}$$

Hence we obtain the following expression for the diffraction efficiency:

$$\eta = |M|^2\frac{\sin^2 X}{X^2}. \tag{4.6}$$

Here M is the strength of the hologram as defined by Eq. (3.4).

4.2. Comparison of the selective properties for different cases

It is easy to verify (see below) that for thin holograms ($L \lesssim \lambda/\theta_{AB}^2$), the dimensionless mismatch X is small, $|X| \ll 1$. This means that for them the effects of shrinkage of the photolayer, and also the spectral or angular shift of the reconstructing wave affect the diffraction efficiency very weakly: the thin hologram acts on any incident wave as a transparency. In this regard one commonly says that thin holograms do not possess selectivity. For this reason they are widely employed in problems of optical information processing and holographic interferometry, where one must vary the parameters of the readout radiation over a wide range.

Now let us proceed to thick-layer holograms. For them the parameter X varies over a broad range, and the diffraction efficiency can depend strongly on the frequency and the direction of the readout wave. The quantity η is not small only when the Bragg condition $X \approx 0$ is satisfied: this property of thick-layer holograms is called spectral-angular selectivity.

The factor $\sin X/X$ in (4.5) is the Fourier image of the coefficient $\tilde{B}\Delta n_{AB}$, which is constant inside the photolayer and equal to zero outside it; actually $A(z=L)$ is given, according to (4.4), by the integral of $\exp(i\Delta kz)$ with respect to dz over the interval from 0 to L. If the coefficient $B\Delta n_{AB}$ is not constant, e.g., owing to absorption during recording and/or during reconstruction, owing to inhomogeneity of the photosensitivity over the depth, etc., then the form of the selectivity curve can be somewhat altered. However, it is important that the width of the central maximum of this curve is determined by the condition $|X| < \pi$. Concretely Eq. (4.6) implies for the width[4)] (according to the criterion of the first vanishing point) that

$$\Delta X\ (\mathrm{FW0M}) = 2\pi. \tag{4.7}$$

Now let us discuss the dependence of the mismatch $X = L\Delta k/2$ on the parameters of the medium and the readout beam.[15,26] For the reconstruction of holograms in which a complex object wave is recorded with an extended angular spectrum, the case is of greatest interest in which the frequency and angle shifts are small, since precisely then are the image distortions small. In this case one can write a rather compact formula that takes simultaneous account of the action of all possible effects by expanding the quantity X in a series to the accuracy of first-order terms in small parameters:

$$X = \frac{\Delta k_z L}{2} = \frac{\omega L}{2c}\,\varepsilon^{1/2}\left\{\left(\nu + \frac{1}{2}\frac{\Delta\varepsilon}{\varepsilon}\frac{1}{\cos\theta_B\cos\theta_A}\right)\times(\cos\theta_A - \cos\theta_B) + \frac{\Delta\omega}{\omega}\left[\cos\theta_B - \frac{1-\varepsilon^{-1}(\mathbf{m}_A\mathbf{m}_B)}{\cos\theta_A}\right] - \frac{1}{\varepsilon}\left(\frac{\mathbf{m}_A}{\cos\theta_A} - \frac{\mathbf{m}_B}{\cos\theta_B}\right)\Delta\mathbf{m}_B\right\}. \tag{4.8}$$

Here we have introduced the quantity ν, which characterizes the variation of z—the scale in the photolayer arising from shrinkage: $L = L_0/(1+\nu)$, so that $\nu > 0$ corresponds to decreased thickness of the photolayer. The parameter $\Delta\omega/\omega = (\tilde{\omega} - \omega)/\omega$ is the relative frequency shift, $\Delta\varepsilon/\varepsilon = (\tilde{\varepsilon} - \varepsilon)/\varepsilon$ is the same for the mean dielectric permittivity. In Eq. (4.8) we use the symbols $\mathbf{m}_A$ and $\mathbf{m}_B$ for the projection of the unit vectors $\mathbf{n}_A^{\mathrm{air}}$ and $\mathbf{n}_B^{\mathrm{air}}$ on the plane of the hologram. The vectors $\mathbf{n}_A^{\mathrm{air}}$ and $\mathbf{n}_B^{\mathrm{air}}$ characterize the directions of propagation of the waves A and B during recording (in air):

$$\mathbf{n}_A^{\mathrm{air}} = \mathbf{m}_A + \mathbf{e}_z(1-\mathbf{m}_A^2)^{1/2}, \qquad \mathbf{n}_B^{\mathrm{air}} = \mathbf{m}_B \pm \mathbf{e}_z(1-\mathbf{m}_B^2)^{1/2}. \tag{4.9}$$

In the second formula of (4.9) the plus sign corresponds to a transmission, and the minus sign to a reflection hologram. The quantity $\Delta\mathbf{m}$ characterizes the change in direction of the readout wave as compared with the direction of the reference wave in recording (both in air):

$$\Delta\mathbf{m} = \tilde{\mathbf{m}}_B - \mathbf{m}_B.$$

The quantities $|\mathbf{m}_A| = \sin\theta_A^{\mathrm{air}}$, $|\mathbf{m}_B| = \sin\theta_B^{\mathrm{air}}$, and $|\mathbf{m}_{\tilde{B}}| = \sin\theta_{\tilde{B}}^{\mathrm{air}}$ are determined by the angles of incidence of the corresponding waves. The directions of the vectors $\mathbf{m}_A$, $\mathbf{m}_B$, and $\mathbf{m}_{\tilde{B}}$, which lie in the plane of the hologram, are fixed by the planes of incidence of the corresponding beams; in the general case these directions do not coincide with one another. The cosines of the angles of refraction also appear in Eq. (4.8) (i.e., inside the photoemulsion): $\cos\theta_A = [1 - (\mathbf{m}_A^2/\varepsilon)]^{1/2}$, and $\cos\theta_B = [1 - (\mathbf{m}_B^2/\varepsilon)]^{1/2}$.

For a given hologram one can consider the quantities ν and $\Delta\varepsilon$ to be fixed constants. Then three variables remain at our disposal: the frequency of the readout wave and the two angles characterizing its direction of propagation. If the direction of readout $\tilde{\mathbf{n}}_B$ is fixed, then the condition $X = 0$ determines the frequency ω of optimal reconstruction. Yet if the frequency ω is fixed, then this condition singles out a cone of directions $\mathbf{n}_B$ (inside the photoemulsion) for which the readout wave is efficiently diffracted by the grating $\exp \times (i\mathbf{Q}\cdot\mathbf{R})$; the axis of this cone coincides with the direction $\mathbf{Q}$. Finally, if we change the direction of readout in the plane $(\mathbf{Q}, \mathbf{k}_B)$, the optimal readout frequency is changed.

Thus holograms recorded in layers of great thickness, $L \gtrsim \lambda/\theta_{AB}^2$, possess spectral-angular selectivity: the hologram extracts from an incident beam having a broad angular and frequency spectrum its own narrow spectral band for every direction.

Let us discuss in greater detail the very interesting limiting cases. Let us turn first to reflection holograms and assume that $\cos\theta_A \approx 1$, $\cos\theta_B = -1$, and $|\mathbf{m}_A|$, $|\mathbf{m}_B| \ll 1$. Then (4.8) transforms into

$$X_{\mathrm{refl}} = \frac{\omega L\varepsilon^{1/2}}{2c}\left(2\nu - \frac{\Delta\varepsilon}{\varepsilon} - 2\frac{\Delta\omega}{\omega} + \frac{(\mathbf{m}_A + \mathbf{m}_B)\Delta\mathbf{m}_B}{\varepsilon}\right). \tag{4.10}$$

Reflection holograms are highly sensitive to shrinkage, which alters ε and the frequency of the readout wave; conversely, their angular selectivity is not so large. The high spectral and small angular selectivity enable one to obtain holograms in the scheme of Denisyuk with high image quality upon reconstruction with white-light sources (of the diaprojector type). The color of the reconstructed image for $\Delta\mathbf{m} = 0$ is determined by the optimal frequency

$\tilde{\omega} \approx \omega[(1+2\nu-(\Delta\varepsilon/\varepsilon)]$, while the spectral width is $\Delta\tilde{\omega}(\mathrm{FWOM}) = \omega\lambda_{\mathrm{med}}/L$, where λ_{med} is the wavelength of the light in the medium. For $L \approx 10\,\mu\mathrm{m}$ and $\lambda_{\mathrm{med}} = \lambda_0/n$, we have the rather narrow reflection band $\Delta\omega/\omega \approx 5\%$. Owing to shrinkage ($\nu > 0$), a hologram recorded with a red neon-helium laser usually yields a yellow-green image upon reconstruction. For reflection holograms with $\mathbf{m}_A = -\mathbf{m}_B$, angular selectivity in the first order in $\Delta\mathbf{m}_B$ is absent and is described only upon taking account of second-order terms in $\Delta\mathbf{m}_B$, which amount to $|\Delta\mathbf{m}_B| \sim (\lambda/L)^{1/2}$.

Another important case is transmission holograms, with $\cos\theta_{A,B}\ 1 - \mathbf{m}_{A,B}^2/2\varepsilon$, and $|\mathbf{m}_{A,B}| < 1$. For these we have

$$X_{\mathrm{trans}} = \frac{\omega L\varepsilon^{1/2}}{2c}\left[\left(\nu + \frac{1}{2}\frac{\Delta\varepsilon}{\varepsilon}\right)\frac{\mathbf{m}_B^2 - \mathbf{m}_A^2}{2\varepsilon} - \frac{\Delta\omega}{\omega}\frac{(\mathbf{m}_A - \mathbf{m}_B)^2}{2\varepsilon} - \frac{(\mathbf{m}_A - \mathbf{m}_B)\,\Delta\mathbf{m}_B}{\varepsilon}\right]. \tag{4.11}$$

We see that the sensitivity to shrinkage and to changes in the permittivity ε and the frequency ω here are weaker than in a reflection hologram of the same thickness by a large factor—of the order of $4/\theta_{A,B}^2$. Thus, when $|\mathbf{m}_{A,B}| \sim \theta_{ab}\varepsilon^{1/2} \sim 0.3$ radian $\approx 15°$ (in air), this factor is 40. With equal absolute values of the angle of incidence, $|\mathbf{m}_A| = |\mathbf{m}_B|$, the planes of the holographic grating are normal to the plane of the hologram. In this case the reflection hologram is sensitive neither to shrinkage nor to changes of ε in all orders in ν and $\Delta\varepsilon$. The spectral selectivity is determined primarily by the period $\Lambda = \lambda_{\mathrm{air}}/|\mathbf{m}_A - \mathbf{m}_B|$ of the interference fringes: $\Delta\omega(\mathrm{FWOM}) = \omega 4\Lambda^2/L\lambda_{\mathrm{med}}$. The angular selectivity of a transmission hologram is the same as in a reflection hologram. In fact, the term proportional to $\Delta\mathbf{m}_B$ has the form: $X_{\mathrm{refl}} = (\omega L/2c\varepsilon^{1/2})(\mathbf{m}_B + \mathbf{m}_A)\,\Delta\mathbf{m}_B$ and $X_{\mathrm{trans}} = (\omega L/2c\varepsilon^{1/2})(\mathbf{m}_A - \mathbf{m}_B)\,\Delta\mathbf{m}_B$ for transmission holograms. We should note the anisotropy of this selectivity. We have already pointed out that under such changes in the direction of the readout wave, for which the vector $\tilde{\mathbf{n}}_B$ inside the photolayer remains on a cone with its axis along the grating vector $\mathbf{Q}$, the Bragg mismatch X is not altered. In Eqs. (4.10) and (4.11) this corresponds to $\Delta\mathbf{m}_B \perp (\mathbf{m}_A + \mathbf{m}_B)$ and $\Delta\mathbf{m}_B \perp (\mathbf{m}_A - \mathbf{m}_B)$, respectively. Conversely, when the readjustment of the angle $\Delta\mathbf{m}_B$ of the readout wave is in the direction toward or away from the object wave, the width of the angular selectivity curve in air for a transmission hologram amounts to $\Delta m_B(\mathrm{FWOM}) = 2\varepsilon^{1/2}\Lambda/L = |\mathbf{m}_A - \mathbf{m}_B|2\Lambda^2/\lambda_{\mathrm{med}}L$.

For a reflection hologram the angular selectivity is also anisotropic (if the beams are not exactly opposed, i.e., if $\mathbf{n}_A \neq -\mathbf{n}_B$). Specifically, the diffraction efficiency varies only upon returning $\mathbf{n}_{\tilde{B}}$ in the plane $(\mathbf{n}_A, \mathbf{n}_B)$, and $\Delta m_B(\mathrm{FWOM}) = 2\varepsilon^{1/2}\Lambda_1/L$, where for a reflection hologram Λ_1 is the period of the intersection of the interference fringes with the boundary of the photolayer.

4.3. Experimental illustration

The spectral and angular selectivity of volume holographic gratings have been studied in numerous experiments. We shall present the results of a recent study,[24] which, on the one hand, illustrates the theoretical material presented above, and on the other hand, shows the close connections of contemporary holography with nonlinear optics.

First we shall make a small lyrical aside on the obtaining of beams having a reversed wave front by the methods of holography. As is well known, when one illuminates a hologram with a reconstructing beam $\tilde{B}$ opposite in direction to the recording reference beam B, i.e., when $\mathbf{k}_{\tilde{B}} = -\mathbf{k}_B$, the hologram reconstitutes a field $\tilde{A}$ that is reversed with respect to the object field during recording: $\tilde{A}(\mathbf{R}) = A^*(\mathbf{R})$, $\mathbf{k}_{\tilde{A}} = -\mathbf{k}_A$. That is, it is the complex conjugate in amplitude-phase structure and at the same time opposite in direction. In the description of this process the term $\delta\varepsilon \propto A^* B \times \exp[-i(\mathbf{k}_A - \mathbf{k}_B)\cdot\mathbf{R}]$ figures instead of the cross-term $\delta\varepsilon \propto AB^* \exp[i(\mathbf{k}_A - \mathbf{k}_B)\cdot\mathbf{R}]$. Here all the results of the previous treatment for the efficiency and selectivity of the hologram stay fully in force with the replacement $\mathbf{k}_A \to -\mathbf{k}_A$, $\mathbf{k}_B \to -\mathbf{k}_B$ and of all amplitudes with their complex conjugates.

In the experiment of Ref. 24 a reflection hologram was recorded with the waves B_{S} and A_{L} incident from opposite sides of an extremely thick ($L = 1$ cm) layer of a photosensitive medium (Fig. 4a). The readout wave B_L was applied in a direction making a small angle $\Delta\mathbf{m}$ with the direction exactly opposite to the reference wave B_{S} during recording.

Figure 4b presents the experimental points for the exposure dependence of the diffraction efficiency. The dependence of η on $(|A_{\mathrm{L}}|^2|B_{\mathrm{S}}|^2)^{1/2}$ proved to be quadratic to a good accuracy, in line with Eqs. (3.4) and (3.5); the different curves correspond to series of experiments with different values of the light-sensitivity coefficient β_2. Figure 4c shows the experimental points for the dependence of η on the angle of antiparallelism defect $|\Delta\mathbf{m}| = \xi$ as it varied in the plane of incidence of the beams A_{L} and B_{S} (*1, 2*) and perpendicular to it (*3*). The solid and dashed lines are drawn according to the corresponding theoretical dependences (4.6) and (4.10). These graphs convincingly demonstrate the agreement of theory and experiment, as well as the anisotropy of the angular selectivity of the hologram.

The experiment of Ref. 24 is a brilliant example of how nonlinear optics and dynamic holography differ only in the language of description. The radiation of a high-power pulsed neodymium laser was used[24] for recording and readout. The waves A_{L} and B_{S} had a frequency difference $\Omega/2\pi = (\omega_{\mathrm{L}} - \omega_{\mathrm{S}})/2\pi \approx 3\times10^9$ Hz, whereby the interference pattern $A_{\mathrm{L}}^* B_{\mathrm{S}} \exp(-2ikz + i\Omega t)$ running at the velocity of sound in the medium (in acetone) effected resonance pumping of a sound wave, which served as the holographic grating. Variation of the frequency difference enabled varying the light-sensitivity coefficient β_2 owing to detuning from the resonance condition of excitation of the sound wave. Readout was performed with the wave B_{L} simultaneously with recording, since the hologram existed only in the presence of recording pulses of duration 3×10^{-8} s. The wave B_{L} was coherent with the wave A_{L}, so that in terms of nonlinear optics the process amounted to stimulated Mandel'shtam-

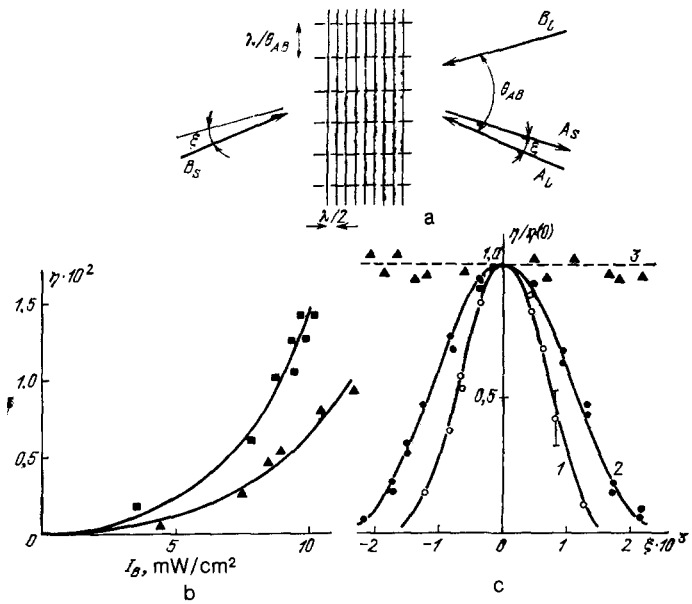

FIG. 4. An experiment[24] to measure angular selectivity. a—Geometry of the interacting beams and orientation of the holographic gratings: ultrasonic grating (solid lines) and effective amplifying grating (dashed line). b—Dependence of the diffraction efficiency on the exposure of the reference wave for different values of the coefficient β_2; solid lines—quadratic parabolas. c—Angular selectivity curves transverse to (dots) and along (triangles) the fringes of the grating for $\theta_{AB} = 4.23\times10^{-2}$ (*1*) and 2.45×10^{-2} (*2*).

Brillouin scattering of the pump field, which consisted of the two waves (A_L and B_L) of frequency ω_L, into the Stokes wave of frequency $\omega_S = \omega_L - \Omega$. As is known, in stimulated scattering for radiation at a Stokes frequency, the medium proves to be amplifying, with an amplification coefficient proportional to the local pump intensity. Thus the process can be described also as follows. The interference of the coherent parallel pump waves A_L and B_L records a transmission hologram $A_L^* B_L$ of the amplification coefficient. The antiparallel Stokes wave B_S, in reading out this hologram, gives rise to the reversed beam $A_S \propto A_L^*$.

Hence one can view the graphs of Fig. 4c as the angular-selectivity curves of a transmission hologram. This fact confirms the important conclusion of the theory that the angular-selectivity curves of reflection and transmission holograms recorded in the same geometry in a layer of fixed thickness coincide.

5. INTRAMODULATIONAL NOISE OF SPECKLE-FIELD HOLOGRAMS

Along with the problem of the diffraction efficiency, one of the central problems in holography is that of the noise in the reconstructed image—the duality of efficiency and quality important now also in other fields. Noise arises from light scattering by the grains of the light-sensitive component of the emulsion, from inhomogeneity of the thickness of the photolayer, and other imperfections of the photomaterial. Specific distortions can arise in imaging holography involving a shift of the reconstructing reference wave in angle and/or frequency as compared with the conditions during recording. In this case, e.g., even in the ideal reconstruction of the object field directly at the output of the hologram, $k\tilde{A}(z=L,\mathbf{r}) = \text{const}\cdot A(z=L,\mathbf{r})$, a frequency shift for the central beams results in a change in the distance to the object. For inclined beams, it leads to distortions like curvature of field and astigmatism. The magnitudes of the shifts prove to differ in different regions of the hologram, and the visible shape of the object is distorted.

An arbitrary object illuminated with a coherent laser beam appears to be covered with small bright spots. That is, the visual image possesses the so-called subjective speckle structure. Since holograms are recorded with coherent radiation, an ideal reconstruction of the object wave conserves this structure, the presence of which is sometimes also regarded as noise in the hologram.

All these forms of real and apparent noise have been repeatedly discussed in the holographic literature, and we shall not deal with them. We shall be interested in the distortion of the object field in the proper sense [i.e., the disagreement of amplitudes of the object waves $A(\mathbf{r})$ and $\tilde{A}(\mathbf{r})$], which is specifically caused by the speckle structure of the object wave in the hologram. They primarily include the intramodulational noise well known in holography.[79] Owing to the inhomogeneities of the intensity of the object speckle wave, intramodulational perturbations of the dielectric permittivity of the form $\beta_1|A(\mathbf{r})|^2$ from (2.9) arise in the hologram. In a thin transmission hologram, $\cos\theta_A \approx \cos\theta_B \approx 1$, these perturbations give rise to an additional spatial phase modulation of the reconstructed field:

$$\tilde{A}(\mathbf{r},\ z=L) = \text{const}\cdot A(\mathbf{r},\ z=L)\, e^{i\varkappa_1|A(\mathbf{r})|^2}\,. \qquad (5.1)$$

Here we have $\varkappa_1 = \omega\beta_+ L/2c\varepsilon^{1/2}$. The inhomogeneity of the phase factor in (5.1) gives just those distortions that are usually called intramodulational.

The question arises of how to characterize quantitatively the quality of reconstruction of the object field? One can naturally try to decompose the entire reconstructed field into a component that exactly reproduces the initial field $A(\mathbf{r})$ and noise. To do this, one should use the projection operation:

$$\tilde{A}(\mathbf{r}) = \frac{A(\mathbf{r})\langle A^*\tilde{A}\rangle}{\langle |A|^2\rangle} + n(\mathbf{r}), \quad \langle A^* n\rangle = 0,$$

Here $n(\mathbf{r})$ is the noise, which by definition is assumed orthogonal to the exact object field.

We shall explain the meaning of this operation with the example of the isolation of the component having a fixed polarization vector $\mathbf{f}$ from depolarized radiation characterized by the dependence of the complex field vector $\mathbf{E}(t)$ on the time t. As is known,[19] here we should take the scalar product $(\mathbf{f}^* \cdot \mathbf{E}(t))$ and find the time-average value of the corresponding intensity $|\mathbf{f}^* \cdot \mathbf{E}|^2/|\mathbf{f} \cdot \mathbf{f}^*|$. The fraction of the energy in the field $\mathbf{E}(t)$ belonging to the polarization $\mathbf{f}$ is $H = |\mathbf{f}^* \cdot \mathbf{E}|^2/(\mathbf{f}^* \cdot \mathbf{f}|\mathbf{E}^* \cdot \mathbf{E}|^2)$; the value of H varies in the range from 1 (for radiation fully polarized parallel to $\mathbf{f}$) to 0 (for radiation orthogonal to $\mathbf{f}$).

Analogously the fraction of the energy H belonging in the field $\tilde{A}(\mathbf{r})$ to the exactly reproducing component $A(\mathbf{r})$ is equal to the normalized scalar product defined in the sense of the overlap integral of the fields over the cross section of the hologram:

$$H = \frac{\left|\int A^*(\mathbf{r})\tilde{A}(\mathbf{r})\,\mathrm{d}^2\mathbf{r}\right|^2}{\left|\int |A(\mathbf{r})|^2\,\mathrm{d}^2\mathbf{r}\right|\left|\int |\tilde{A}(\mathbf{r})|^2\,\mathrm{d}^2\mathbf{r}\right|}. \tag{5.2}$$

This definition of the reproduction fraction H was introduced in Ref. 25 in connection with the problem of the quality of reversal of a wave front. Correspondingly the quantity $1 - H$ is the fraction of the energy belonging to distortions.

The concept that we used above of the scalar product, i.e., the complex overlap integral $\int A^*(\mathbf{r}, z_0)\tilde{A}(\mathbf{r}, z_0)\,\mathrm{d}^2\mathbf{r}$ of the two slow amplitudes A and $\tilde{A}$ of the fields

$$A(\mathbf{r}, z)\exp(-i\omega t + i\mathbf{k}_A\mathbf{R})$$

$$\text{and } \tilde{A}(\mathbf{r}, z)\exp(-i\tilde{\omega}t + i\mathbf{k}_{\tilde{A}}\mathbf{R})$$

has the following important property. If $\omega = \tilde{\omega}$ and $\mathbf{k}_A = \mathbf{k}_{\tilde{A}}$, i.e., the frequencies and central directions of propagation coincide, then the slow amplitudes satisfy the same equation. Then, in the absence of absorption, their scalar product does not vary in the process of propagation. This enables us to calculate the distortions of the field in the image plane of interest to us from the overlap integral of the fields $\tilde{A}$ and A directly at the output of the hologram.

The noise or distortions bearing the fraction of the energy $1-H$ of the reconstructed object beam are manifested in different ways in different systems of recording holograms. First let us study the example of using a hologram for recording information, which is represented as a block of dark and light sites in a transparency illuminated with a plane, coherent wave. Then during reconstruction a coherent noise increment will arise in the image of the transparency having the mean intensity $(1 - H)I_A$, where I_A is the average over the cross section of the intensity of the reconstructed wave. At the dark spots of the original image, the noise yields a background speckle-inhomogeneous illumination, $I_{\text{noise}} = (1 - H)\,I_A$. In contrast, the interference of the noise with the main field at the bright spots of the image leads to an additional modulation of the intensity with a range of $\Delta I/I \sim 4(1 - H)^{1/2}$. Thus, with a noise fraction of only $1 - H \approx 0.04$, the range of the interference modulation becomes of the order of $\Delta I/I \sim 0.8$, i.e., of the order of 100%, and the quality of the reconstructed image is completely unsatisfactory.

Another example is imaging holography. Here the field itself of the object illuminated with coherent laser light has a speckle structure. However, the information subjectively perceived by the observer is contained not in the details of realization of the speckle structure, but in the general shape of the object and the intensity of illumination of the different parts of it. In the illuminated region of the object, the interference of the noise with the signal will change only the realization of the speckle pattern. Therefore the role of the noise is reduced only to a background illumination having the energy $(1 - H)\,I_A$, which is approximately uniformly distributed over the field of the image. That is, contrast is reduced. Thus, in imaging holography this noise is manifested far more weakly, as $(1 - H)$, than in coherent-optical systems, where its role is estimated by the parameter $4(1 - H)^{1/2}$.

In the presence of noise in the reconstructed wave, one should define more accurately what is called the diffraction efficiency. Let us denote by η the ratio of all the energy reconstructed by the hologram in the direction of the image of the object to the incident energy of the reference wave. Moreover, we shall denote by η_0 the energy of the component of the reconstructed field that exactly reproduces the original object wave $A(\mathbf{R})$, also referred to the input energy. We can easily understand that the overall diffraction efficiency η, the efficiency of diffraction into the exact image η_0, and the reproduction fraction H are connected by the relationship $\eta_0 = H\eta$.

Evidently a rigorous definition of these quantities for holograms of speckle fields must contain an averaging over the cross section of the hologram. By analogy with (3.4), and with (5.2) in mind, we shall write

$$\eta = \frac{\langle|\tilde{A}|^2\rangle}{|\tilde{B}|^2}\frac{S_A}{S_B}, \quad \eta_0 = \frac{|\langle\tilde{A}A^*\rangle|^2}{|\tilde{B}|^2\langle|A|^2\rangle}\frac{S_A}{S_B}. \tag{5.3}$$

For a field $A(\mathbf{R})$ distorted according to the law (5.1), the overlap integral from (5.2) can be calculated when the field $A(\mathbf{r})$ is statistically uniform by replacing the spatial integration with an equivalent averaging over the ensemble of realizations of speckle fields. This yields

$$1 - H = \frac{\eta - \eta_0}{\eta} = 1 - \frac{(1 + 2I_A\,\mathrm{Im}\,\varkappa_1)^2}{|1 - iI_A\varkappa_1|^4}$$

$$\approx 2\,|\varkappa_1|^2 I_A^2 L^2 = 2\eta\frac{I_A}{I_B}\left|\frac{\beta_1}{\beta_2}\right|^2. \tag{5.4}$$

The approximate equality in (5.4) corresponds to the case of low noise, while the last of the equalities of (5.4) has been written by using the Born expression (3.4) for the diffraction efficiency η of the ratio of mean intensities of the waves I_A/I_B in recording and the ratio $|\beta_1/\beta_2|$ of the transfer coefficients for the intra- and cross-perturbations. The coefficient "2" (Gaussian doubling) in (5.4) arises from the fact that the noise phase shifts are large precisely wherever the amplitude of the object field is large. We see that the relative noise level in the image increases linearly with increasing η (so that the absolute intensity of the noise increases as η^2). Equation (5.4) implies that the intramodulation noise decreases as (I_A/I_B) approaches zero, i.e., if we

take a reference wave with an intensity appreciably greater than the object wave during recording.

A rather widespread method for decreasing the noise in the image is spatial filtration using cutoff diaphragms. This method allows one to eliminate only those angular components of the noise that lie outside the angular spectrum of the object wave. In this connection we should stress that the intramodulational distortions for $\varkappa_1|A|^2 \lesssim 1$ lie approximately within the angular spectrum of the object field itself, and this noise cannot be removed by stopping down.

Now let us discuss the features of the intradistortions in thick-layer holograms. Intraperturbations of the dielectric permittivity $\delta\varepsilon(\mathbf{R}) = \beta_1|A(\mathbf{R})|^2$ lead to two effects in them. They are, first, a modulation of the phase of the reconstructed wave. As an accurate treatment performed with Eqs. (4.5) and (4.8) shows, the phase modulation in thick-layer holograms (both transmission and reflection) has the form (5.1) with the replacement $L \to (L/2)[(\cos\theta_A)^{-1} + |\cos\theta_B|^{-1}]$. Second, the change in the refractive index leads to a departure from the Bragg condition

$$\delta X = \delta n_{in}(\mathbf{r}) \frac{\omega L}{2c}\left(\frac{1}{\cos\theta_A} - \frac{1}{\cos\theta_B}\right) \tag{5.5}$$

and to a local change in the amplitude of the reconstructed field according to a $\sin X/X$ law.

Actually the second effect proves substantial only for reflection holograms, where we have $(\cos\theta_A)^{-1} - (\cos\theta_B)^{-1} \approx 2$. Moreover, when $X_0 = 0$, the function $(\delta X)^{-1}\sin\delta X$ behaves like $1 - [(\delta X)^2/6] + O((\delta X)^4)$, so that the contribution of the amplitude effect will be appreciable only in the case of strong modulation, $\varkappa|A(\mathbf{r})|^2 \sim 1$.

Finally, let us turn to the intranoise in volume holograms. Here several lengths of the speckle element of the object field fit into the thickness L of the hologram, $L/\Delta z_A > 1$. Let us make a crude estimate of the intradistortions, assuming: 1) that they consist only in phase distortion of the field, and 2) that we can take this phase in the form of an integral of the perturbations along the ray:

$$\tilde{A}(\mathbf{r}) \approx A(\mathbf{r}) \exp\left[i\frac{\omega l}{c}\int_0^L dz\, \delta n(\mathbf{r}, z)\right]. \tag{5.6}$$

The quantity $\delta n(\mathbf{r}, z) = \beta_1|A(\mathbf{r}, z)|^2/2\varepsilon_0^{1/2}$ that appears in the integrand in (5.5) contains both the space-average component $\delta n \propto \langle|A|^2\rangle$ and the component fluctuating in time with the local fluctuations $|A(\mathbf{r}, z)|^2 - \langle|A|^2\rangle$ of the intensity of the speckle field. The former component gives a phase factor constant over the cross section, and does not lead to distortions. The fraction of distortions $1 - H$ arises from the fluctuating component of the phase and is equal to

$$1 - H \approx \eta \frac{I_A}{I_B}\left|\frac{\beta_1}{\beta_2}\right|^2 \frac{\Delta z_A}{L}. \tag{5.7}$$

The small factor $\Delta z_A/L$ characterizes the partial compensation of the sign-varying fluctuations of the phase shift from the speckle elements through which the ray passes. An exact calculation of the intramodulational noise (see Sec. 11) does not alter the structure of the answer (5.7) and only concretizes the value of the parameter $\Delta z_A/L$.

Thus, other conditions being the same, the magnitude of the intramodulational noise for volume holograms of speckle fields is smaller than for thin and thick-layer holograms of speckle fields by a factor $L/\Delta z_A$, which equals the number of speckle elements per thickness of the photoemulsion.

6. EFFECT OF SATURATION OF THE PHOTORESPONSE

Owing to the limited dynamic range of real recording media, the approximation (2.9) of a linear relationship between the photoresponse $\delta\varepsilon$ and the local intensity I of the recording radiation $\delta\varepsilon = \beta I$ has a rather narrow range of applicability. We shall study the saturation of the photoresponse of real media in the model of a two-parameter exposure curve of the form[34]

$$\delta\varepsilon(I) = \beta I_{sat}(1 - e^{-I/I_{sat}}). \tag{6.1}$$

This expression describes well the actually used photomaterials PE-2, LOI-2, VRL, and IAE[30]; here I_{sat} is the intensity corresponding to a saturating exposure of the medium for the given exposure time. The coefficient β characterizes the light-sensitivity of the medium when $I \ll I_{sat}$; in this limit the previously introduced coefficients β_1 and β_2 [Eq. (2.9)] coincide in this model: $B_1 = \beta_2 = \beta_1$; see also Refs. 80 and 81.

An important characteristic of a photolayer that determines its potentialities is a quantity that we can call the saturability parameter of the photolayer. Following the notation of Eq. 30, we shall write it in the form $\varphi_0^{-1} = (\varkappa I_{sat})^{-1}$. Numerically it is equal to the reciprocal of the maximum phase advance $\varkappa I_{sat}$ induced in the medium by a large exposure $I \gg I_{sat}$, $\delta\varepsilon \approx \beta I_{sat}$.

In comparison with linear materials (for which $\varphi_0^{-1} \to 0$) having the same light sensitivity β, the efficiency of recording of cross- and intrainhomogeneities is reduced in a saturating photolayer. Moreover, the fringe profile of the holographic grating becomes nonsinusoidal. This further reduces its efficiency of readout, while in thin holograms it can lead to the appearance of higher orders of diffraction. In order to discuss these effects quantitatively, we shall represent (6.1) as a sum of harmonics of the holographic grating:

$$\delta\varepsilon(\mathbf{R}) = \delta\varepsilon_{in}(\mathbf{R}) + 2\delta\varepsilon_{cr}(\mathbf{R})\cos(\mathbf{QR} + \varphi) + \sum_{n=2}^{\infty}\delta\varepsilon^{(m)}\cos(n\mathbf{QR} + n\varphi). \tag{6.2}$$

The local amplitudes of the intramodulational component $\delta\varepsilon_{in}(\mathbf{R})$ and the first harmonic of the grating $\delta\varepsilon_{cr}(\mathbf{R})$ are determined here by the local amplitude of the speckle field $|A(\mathbf{R})|$:

$$\delta\varepsilon_{in} = \beta I_{sat}\left[1 - I_0\left(2\frac{|AB|}{I_{sat}}\right)\exp\left(-\frac{|A|^2 + |B|^2}{I_{sat}}\right)\right],$$

$$\delta\varepsilon_{cr} = \beta I_{sat}\left(2\frac{|AB|}{I_{sat}}\right)\exp\left(-\frac{|A|^2 + |B|^2}{I_{sat}}\right). \tag{6.3}$$

In the relationships of (6.3) I_0 and I_1 are modified Bessel functions.

In this section we shall restrict the treatment to thin- and thick-layer holograms with $L \lesssim \lambda/\Delta\theta_A^2$, so that the am-

plitudes $\delta\varepsilon_{\rm in}(\mathbf{r})$ and $\delta\varepsilon_{\rm cr}(\mathbf{r})$ can be considered constant throughout the depth of the photolayer. Figure 5 shows the relationships of the local strengths of the hologram $M = (\varkappa/\beta)\delta\varepsilon_{\rm cr}$ and the intramodulational phase advance $\Psi = (\varkappa/\beta)\delta\varepsilon_{\rm in}$ on the parameter $M_0 = \varkappa|AB|$ proportional to the exposure; M_0 is numerically equal to the strength of the hologram in a layer of the same photosensitivity β, but with a linear response. The parameters are given for differential local values of the ratio of intensities of the recording waves $|A(\mathbf{R})|^2/I_B$ and are expressed in units of φ_0.

As we see from Fig. 5, the phase advance Ψ in the large-exposure limit approaches the maximum possible value φ_0. In contrast, the strength of the hologram M for large exposures approaches zero asymptotically, but passes through a maximum when $M_0 \sim \varphi_0$. The maximum value of the strength of the hologram is determined by the saturability parameter of the photolayer φ_0^{-1} and the ratio $|A|^2/|B|^2$. The requirement for high diffraction efficiency of the hologram is restricted by the attainable values of the parameters φ_0^{-1}. Thus, for example, one can attain $M \approx \pi/2$, and record a transmission phase hologram with maximal diffraction efficiency only in weakly saturable layers, $\varphi_0^{-1} \lesssim 0.14$. We note also that the optimal recording from the standpoint of efficiency of reconstruction is obtained with waves of equal intensity, since under these conditions the relative level of the background illumination $\varkappa(|A|^2 + |B|^2)$ saturating the photolayer is minimal.

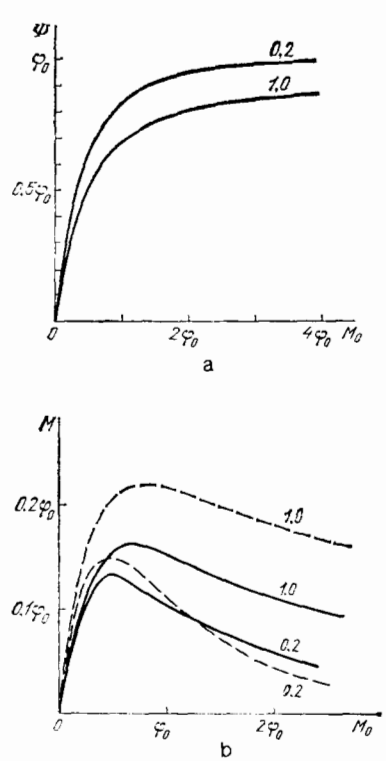

FIG. 5. a—Dependence of the phase advance ψ in a hologram of plane waves on M_0 for the different values of $I_A/I_B = 1; 0.2$. b—Dependence of the strength M of the hologram on M_0 in a hologram of plane waves (dashed lines) and in a volume speckle hologram (solid lines) for the different values $I_A/I_B = 1$ and 0.2.

In the Born approximation when the Bragg condition $X = 0$ is satisfied throughout the area of the hologram, the local amplitude of the reconstructed wave now has the form:

$$\tilde{A} = iM\frac{AB^*}{|AB|}e^{i\Psi}\tilde{B}, \quad M = \frac{\varkappa}{\beta}\delta\varepsilon_{\rm cr}, \quad \Psi = \frac{\varkappa}{\beta}\delta\varepsilon_{\rm in}. \tag{6.4}$$

Here $\delta\varepsilon_{\rm cr}$ and $\delta\varepsilon_{\rm in}$ are defined in (6.3). Equation (6.4) is valid at low diffraction efficiency, i.e., when $|M| < 1$. However, applying it to the case of reflection holograms requires the additional condition of small fluctuations of the Bragg mismatch $|\delta X| = |\delta\Psi| \lesssim 1$ owing to the intramodulational inhomogeneities $\delta\varepsilon_{\rm in}$ $(|A|^2)$. This condition ensures that the Bragg condition will be satisfied at all points. Moreover, for thin holograms (6.4) is applicable only if the fraction of the energy of the readout wave scattered into the higher diffraction orders is small.

First we shall estimate the effect of the intramodulational factor $e^{i\Psi}$. We shall do this by expanding the expression (6.3) for $\delta\varepsilon_{\rm in}$ up to first-order terms in the parameter $I_A/I_{\rm sat}$:

$$\langle\Psi\rangle \approx \varphi_0(1 - e^{-I_B/I_{\rm sat}}),$$
$$\langle|\delta\Psi|^2\rangle \approx \left(1 - \frac{I_B}{I_{\rm sat}}\right)^2 e^{-2I_B/I_{\rm sat}}|\varkappa I_A|^2. \tag{6.5}$$

At low exposures $I_B \ll I_{\rm sat}$ the relative level of intramodulational distortions is the same as in unsaturated recording: $\langle|\delta\Psi|^2\rangle \sim |\varkappa I_A|^2$. Saturation strongly lowers the efficiency of recording of the intramodulational inhomogeneities. Consequently the relative level of distortions, as we can easily obtain from (6.5), reaches the maximum

$$\langle|\delta\Psi|^2\rangle_{\max} \sim 2.5\cdot 10^{-2}\varphi_0^2\left(\frac{I_A}{I_B}\right)^2 \quad \text{when} \quad I_B \approx 0.4\, I_{\rm sat}.$$

It even declines with further increase in exposure. Thus, in the real situation with $\varphi_0 \lesssim 10$ and $I_A \lesssim 0.3\, I_B$, the intramodulational distortions are small. Therefore we shall calculate the quantities η and η_0 from (5.3), neglecting the intramodulation factor, and applying averaging over the ensemble of speckle fields:

$$\eta = \frac{|\varphi_0|^2}{1+(2I_A/I_{\rm sat})}I_1\frac{2I_AI_B}{I_{\rm sat}(I_{\rm sat}+2I_A)}\exp\left[-\frac{2I_B(I_{\rm sat}+I_A)}{I_{\rm sat}(I_{\rm sat}+2I_A)}\right], \tag{6.6}$$

$$\eta_0 = \frac{|\varkappa|^2 I_AI_B}{[1+(I_A/I_{\rm sat})]^4}\exp\left(-\frac{2I_B}{I_{\rm sat}+I_A}\right). \tag{6.7}$$

In the presence of an appreciable amplitude component in the photoresponse $\operatorname{Im}\beta \neq 0$, one should multiply the right-hand sides of (6.6) and (6.7) by the factor $\exp(-\operatorname{Im}\langle\Psi\rangle)$, which describes the mean light-induced absorption.

Figure 6 shows the relationships of η and η_0 to M_0 for different fixed values of I_A/I_B. We note first of all the universal character of the dependences of the diffraction efficiencies on the exposure. Photomaterials of differing chemical composition, layer thickness, and processing regime have completely different parameters. However, in the Born approximation, i.e., for small η and η_0, for all of them the dependences of the diffraction efficiency divided by φ_0^2 on

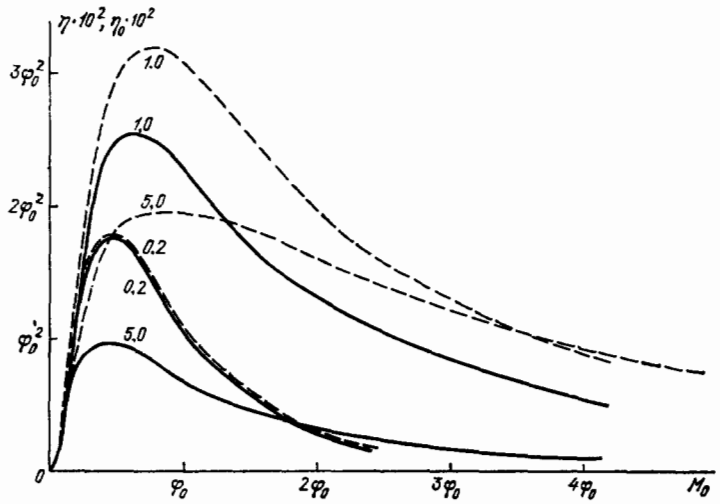

FIG. 6. Universal dependences of η (dashed lines) and η_0 (solid lines) on M_0 for the different values $I_A/I_B = 0.2$, 1, and 5 in a photolayer having the saturability φ_0^{-1}.

the exposure (or more exactly, on $M_0/\varphi_0 = (I_A\, I_B/I_{\rm sat}^2)^{1/2}$ are the same.

The quantities η and η_0 differ appreciably when $I_A > I_B$. The cause of the noise in this case is not the phase modulation of the field by the intrainhomogeneities, but the nonlinearity of the dependence of the local modulus of the amplitude of the reconstructed wave $|\widetilde{A}(\mathbf{r})| \propto M(\mathbf{r})$ on the modulus of the recorded $|A(\mathbf{r})|$. Noise of this type, which corresponds to reproduction of the phase profile, but distortion of the amplitude profile of the field in the cross-section of the hologram, will be called cross-modulational. In the opposite case in which the mean intensity of the object wave is appreciably smaller than the intensity of the reference wave, the cross-modulational noise is just as small as the intramodulational noise, and the $\eta(M_0)$ and $\eta_0(M_0)$ relationships practically coincide. Numerical calculations by the exact formulas for phase photolayers with $\varphi_0 = 1$ have shown that the relationships of Fig. 6 found neglecting the factor $e^{i\Psi}$ yield deviations from the exact values by no more than a few percent.

Now we shall discuss the maximum values of the diffraction efficiencies. The maximum of η_0 is reached at $(I_A I_B)^{1/2}/I_{\rm sat} = \{[1 + 4(I_A/I_B)^2]^{1/2} - 1\}/2(I_A/I_B)^{3/2}$. For $I_A/I_B \lesssim 0.3$, this corresponds to the condition $I_B \approx I_{\rm sat}$ found in Ref. 30. The maximum value itself of the diffraction efficiency in this limit $I_A \lesssim 0.3\, I_B$ is determined by the expression

$$\eta^{\max} \approx \eta_0^{\max} \approx \varphi_0^2 \frac{I_A/I_B}{[1+(I_A/I_B)]^4} \exp\left(-\frac{2I_B}{I_A+I_B}\right), \quad (6.8)$$

That is, it is unambiguously expressed in terms of the magnitude of the saturability parameter φ_0^{-1} and the ratio of intensities of the recording beams. For each specific layer characterized by the saturability parameter φ_0^{-1}, the maximum efficiencies of holograms of speckle fields correspond to the condition $I_A \approx I_B$: $\eta^{\max} \approx 3.2\times 10^{-2}\varphi_0^2$) $\eta_0^{\max} \approx 2.55 \times 10^{-2}\varphi_0^2$.

We must stress that, although the obtained results are approximate in nature, their limits of applicability are very broad and correspond to typical experimental conditions. We shall assume that the Born approximation is valid when $\eta < 10\%$. As we see from Fig. 6, for photolayers with $\varphi_0^{-1} \gtrsim 0.5$ this is true only for any I_A/I_B relationships and exposures. For photolayers of lower saturability this approximation is valid throughout the entire range of exposures for $I_A/I_B \lesssim 0.74\varphi_0^{-2}$.

7. DIFFRACTION OF LIGHT BY SINUSOIDAL GRATINGS

Thus far we have been treating holograms of low diffraction efficiency, restricting the treatment to the first Born approximation of the theory of scattering by cross perturbations. It is convenient to start the discussion of holograms of high diffraction efficiency (of the order of unity) with the example of strictly periodic holographic gratings, i.e., holograms recorded by the interference of two plane waves.

7.1. Thin hologram

We shall take the transmission coefficient of a thin holographic grating in the form

$$t(\mathbf{r}) = \exp\,[i\Psi + 2iM\cos(\mathbf{Qr} + \varphi)]. \quad (7.1)$$

Here $\mathbf{q} = (\mathbf{k}_A - \mathbf{k}_B)$ is the wave vector of the grating in the plane of the hologram, $\varphi = \arg(AB^*)$, A and B are the amplitudes of the plane waves during recording, M is the strength of the hologram [see (3.5)], and

$$\Psi = \varkappa_1(|A|^2 + |B|^2), \quad M = \varkappa_2 |A||B|, \quad (7.2)$$

$$\varkappa_{1,2} = \frac{\beta_{1,2}\omega L}{2ce^{1/2}}.$$

Let us use the well-known formula

$$e^{i\rho\cos\gamma} = \sum_{n=-\infty}^{+\infty} i^n J_n(\rho)\, e^{in\gamma},$$

where $J_n(z)$ is a Bessel function. Then we can easily obtain the energy distribution over the different diffraction orders. In particular, in first-order diffraction, which corresponds as if to an reconstructed object wave, we have

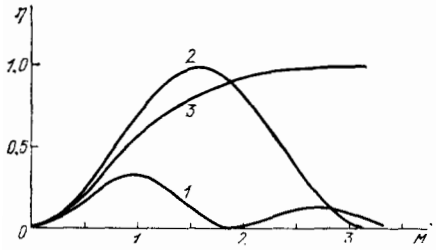

FIG. 7. Dependences of the diffraction efficiencies of thin (*1*), thick-layer transmission (*2*), and reflection (*3*) phase holograms of plane waves on the strength M of the grating.

$$\tilde{A} = \frac{AB^*}{|AB|}\tilde{B}i\exp(i\Psi)J_1(2M),$$
$$\eta = \exp(-2\,\mathrm{Im}\,\Psi)\,|J_1(2M)|^2. \tag{7.3}$$

For pure phase holograms we have $\mathrm{Im}\,\Psi = \mathrm{Im}\,M = 0$ and $\eta = J_1^2(2M)$ (Fig. 7). For small values of the argument $2M$ in (7.3) for a phase hologram, we obtain the result of the first Born approximation, $\eta = M^2$. The value of the function $J_1^2(2M)$ reaches its absolute maximum at $2M = 1.8$ and is $\eta_{\max} \approx 34\%$. With further increase in the strength of the hologram M the diffraction efficiency gradually declines while oscillating toward zero. The reason for this decline involves the outflow of energy into other diffraction orders.

7.2. Theory of two coupled waves

Now let us examine a hologram recorded by two plane waves in a photolayer of rather large thickness, $L \gg \lambda/\theta_{AB}^2$. In this case the higher orders of diffraction do not satisfy the Bragg condition and hence are not excited. Thus, even for a minimal wave mismatch X_{-1} in diffraction into the minus-first order, we have $X_{-1} \sim L\theta_{AB}^2/\lambda \gg 1$. Consequently only two waves are present in the volume of the hologram in the process of reconstruction: the reference wave $\tilde{B}(z)\exp(i\mathbf{k}_{\tilde{B}}\cdot\mathbf{R})$ and the object wave $\tilde{A}(z)\exp[i(\mathbf{k}_{\tilde{B}} + \mathbf{Q})\cdot\mathbf{R}]$. When the diffraction efficiency is high, we must take account of the change of amplitude of the reference wave $\tilde{B}$ due to outflow of energy into the object beam $\tilde{A}$, i.e., treat the self-consistent process including both scattering processes, $\tilde{B}\to\tilde{A}$ and $\tilde{A}\to\tilde{B}$, in the holographic grating. Thus we arrive at the problem of determining the z-dependent slow amplitudes $a(z)$ and $b(z)$ of the two coupled waves:

$$\tilde{E}(\mathbf{R}) = \frac{b(z)}{|\cos\theta_B|^{1/2}}\frac{B}{|B|}\exp(i\mathbf{k}_{\tilde{B}}\mathbf{R}) + \frac{a(z)}{(\cos\theta_A)^{1/2}}\frac{A}{|A|}\exp[i(\mathbf{k}_{\tilde{B}} + \mathbf{Q})\mathbf{R}]. \tag{7.4}$$

We can obtain the truncated equations for the amplitudes $a(z)$ and $b(z)$ from the wave equation (3.1) with $\delta\varepsilon(\mathbf{R})$ from (2.9). To do this, just as in deriving Eq. (3.3), we must neglect the terms $\sim d^2a/dz^2, d^2b/dz^2$, and the higher orders of diffraction. Then we obtain

$$\frac{da}{dz} - i2\frac{X}{L}a(z) = i\frac{M}{L}b(z), \quad \pm\frac{db}{dz} = i\frac{M}{L}a(z). \tag{7.5}$$

Here in the second equation the (+) sign corresponds to a transmission hologram, and (−) to a reflection hologram.

The parameter X characterizes the mismatch from the Bragg condition; see (4.8). The seeming asymmetry of the equations (7.5) with respect to the $a \leftrightarrows b$ substitution involves the fact that we have written the exponential factors in (7.4) in different ways (asymmetrically). The boundary conditions have the form $a(z=0) = 0$, $b(z=0) = 1$ for transmission holograms or $a(z=0) = 0$, $b(z=L) = \exp[-i(\mathbf{k}_{\tilde{B}}\cdot\mathbf{e}_z)L]$ for reflection holograms. In both cases we are interested in the complex amplitude of the reconstructed object wave at the output of the hologram, $a(z=L)$, in terms of which the diffraction efficiency is expressed, $\eta = |a(z=L)|^2$.

The solution of the system (7.5) gives

$$\eta_{\text{trans}} = \frac{M^2\sin^2(X^2+M^2)^{1/2}}{X^2+M^2},$$
$$\eta_{\text{refl}} = \frac{M^2\sin^2(X^2-M^2)^{1/2}}{X^2-M^2\cos^2(X^2-M^2)^{1/2}}. \tag{7.6}$$

For the sake of definiteness, here we have restricted the treatment to the case of pure phase holograms. For reflection holograms we must take account of the fact that $\sin^2(X^2-M^2)^{1/2} = -\sinh^2(M^2-X^2)^{1/2}$ and $\cos^2(X^2-M^2)^{1/2} = \cosh^2(M^2-X^2)^{1/2}$. The notation in terms of hyperbolic functions is more convenient when $M > |X|$. For arbitrary amplitude-phase holograms the answer can be found in Refs. 12 and 26.

Under optimal readout conditions, $X = 0$, the diffraction efficiency is maximal and depends as follows on the strength M of the hologram: $\eta_{\text{trans}} = \sin^2 M$, $\eta_{\text{refl}} = \tanh^2 M$ (see Fig. 7). In a phase transmission hologram with $M = \pi/2$, one obtains 100% pumping of the energy from the reference wave into the object wave. With further increase in M the efficiency diminishes owing to pumping of energy back into the reference wave. The amplitudes of the interacting waves vary inside the photolayer according to the law

$$b(z) = b(0)\cos\frac{Mz}{L}, \quad a(z) = -ib(0)\sin\frac{Mz}{L}. \tag{7.7}$$

In a reflection hologram one also attains practically complete pumping of the energy, and η_{refl} monotonically approaches unity with increasing M. The corresponding amplitudes $a(z)$ and $b(z)$ vary through the depth of the photolayer according to the law

$$b(z) = \frac{b(L)\,\mathrm{ch}(Mz/L)}{\mathrm{ch}\,M}, \quad a(z) = \frac{ib(L)\,\mathrm{sh}(Mz/L)}{\mathrm{ch}\,M}. \tag{7.8}$$

Below in Sec. 8 we shall need expressions for the complex amplitude of the reconstructed field $A(z=L)$ for calculating the distortions in thick-layer holograms of speckle fields. While keeping only the $\tilde{A}(A)$ relationship of interests to us, we obtain the following from the system (7.5) with account taken of (7.4) and the boundary conditions:

$$\tilde{A}(z=L)_{\text{trans}} = \text{const}\cdot\frac{A}{|A|}\frac{M\sin(M^2+X^2)^{1/2}}{(M^2+X^2)^{1/2}} \times \exp[i\varkappa_1(|A|^2+|B|^2)], \tag{7.9}$$

$$\tilde{A}(z=L)_{\text{refl}} = \text{const}\cdot\frac{A}{|A|}\frac{M}{(M^2-X^2)^{1/2}\,\mathrm{cth}\,(M^2-X^2)^{1/2} - iX}. \tag{7.10}$$

For transmission holograms we have introduced here the parameter $\varkappa_1 = (\omega\beta_1 L/4c\varepsilon^{1/2})(\cos^{-1}\theta_A + \cos^{-1}\theta_B)$. It differs slightly from $\varkappa_1$ from Eq. (5.1).

8. THIN AND THICK-LAYER HIGH-EFFICIENCY HOLOGRAMS

Thin and thick-layer holograms of speckle fields can be mentally divided into regions whose transverse dimensions are smaller than the dimension of a speckle element. Within the limits of such a region we can treat the object field as a piece of a plane wave with a certain amplitude and phase, while considering the holographic grating to be regular. Within each region the reconstruction process is described by the model of a hologram of plane waves presented in the preceding section 7.2, and we should take the local value of the slow amplitude $A(\mathbf{r})$ of the speckle field at the given point as the amplitude of the "plane" wave A in making the recording.

8.1. Recording without saturation of the photoresponse

The dependence of the amplitude of the reconstructed wave on the coordinates $\mathbf{r} = (x,y)$ in the exit plane $z = L$ of the hologram is given by Eqs. (7.3) for thin holograms, (7.9) for thick-layer transmission holograms, and (7.10) for thick-layer reflection holograms. Here $|A(\mathbf{r})|^2$, $M(|A(\mathbf{r})|)$, and $X(|A(\mathbf{r})|)$ prove to be functions of the transverse coordinates, which depend on the concrete realization of the speckle structure of the field $A(\mathbf{r})$. These formulas enable one to calculate the overall diffraction efficiency η, the diffraction efficiency η_0 into the exact image, and thus the reproduction fraction $H = \eta_0/\eta$. The averages over the cross-section that figure in the definitions of η, η_0, and H can be replaced for a statistically uniform speckle field $A(\mathbf{r})$ by the averages over the ensemble of speckle fields, i.e., over the probability distribution of (2.2).

The final answer has the following form[27]:

1) *Thin transmission holograms*:

$$\eta = I_1\left(\frac{2|M|^2}{1+2\,\mathrm{Im}\,F_A}\right)(1+2\,\mathrm{Im}\,F_A)^{-1} \times \exp\left[-2\,\mathrm{Im}\,F_B - 2\frac{(\mathrm{Re}\,M)^2-(\mathrm{Im}\,M)^2}{1+2\,\mathrm{Im}\,F_A}\right], \quad (8.1)$$

$$\eta_0 = \frac{|M|^2}{|1-iF_A|^4}\exp(-2\,\mathrm{Im}\,F_B)\left|\exp\left(-\frac{M^2}{1-iF_A}\right)\right|^2. \quad (8.2)$$

Here we have $F_A = \varkappa_1 I_A$, $F_B = \varkappa_1 I_B$, $I_1(z)$ is the modified Bessel function, and $M = \varkappa_2(I_A I_B)^{1/2}$ is the strength of the hologram; for media having a general amplitude-phase response, the quantities F_A, F_B, and M are generally complex.

In the important special case of pure phase holograms, these formulas acquire a simpler form:

$$\eta = I_1(2M^2)e^{-2M^2}, \quad \eta_0 = \frac{M^2}{(1+F_A^2)^2}\exp\left(-\frac{2M^2}{1+F_A^2}\right). \quad (8.3)$$

Here the quantity $I_A = \langle|A|^2\rangle$ is the mean intensity of the object speckle field during recording.

2) *Thick-layer transmission holograms*. For this case it was shown in Sec. 4 that the magnitude of the Bragg mismatch X is practically independent of the intensity of the object field $|A|^2$. Therefore we can assume to a very good accuracy here that X does not depend on the transverse coordinates. For the very interesting case $X = 0$ we have

$$\eta = \frac{\exp(-2\,\mathrm{Im}\,F_B)}{1+2\,\mathrm{Im}\,F_A}\left(Xe^{-X^2}\int_0^X e^{t^2}\,dt + Ye^{Y^2}\int_0^Y e^{-t^2}\,dt\right), \quad (8.4)$$

$$\eta_0 = \frac{|z^2|^2\exp(-2\,\mathrm{Im}\,F_B)}{|1-iF_A|^3}\left|1+\frac{1-2z^2}{z}e^{-Z^2}\int_0^Z e^{t^2}\,dt\right|^2. \quad (8.5)$$

Here we have $X = \mathrm{Re}M(1+2\mathrm{Im}F_A)^{-1/2}$, $Y = \mathrm{Im}\,M(1+2\,\mathrm{Im}\,F_A)^{-1/2}$, $Z = 1/2\,M(1-iF_A)^{-1/2}$, and $F_{A,B} = I_{A,B}/\cos\theta$. For the sake of definiteness we assume that $\cos\theta_A \approx \cos\theta_B \approx \cos\theta$.

3) *Thick-layer reflection holograms*. Here one can perform an explicit analytic calculation[27] of the quantities η and η_0 only in the case in which one can assume $X = 0$ throughout the hologram. Since for reflection holograms the Bragg mismatch X is far more sensitive to intraperturbations, the approximation $X = 0$ would be valid only when $\beta_1^{1/2}|A|^2 \ll \beta_2^{1/2}|B|^2$. For this reason we shall present only the results of an exact numerical calculation. All the expressions derived in Ref. 27 and given above are valid for arbitrary amplitude-phase recording media. Figure 8 shows the dependences of the quantities η and η_0 on the strength of the phase hologram M_0. Here the averaging of Eqs. (7.3), (7.9), and (7.10) over the probability distribution of (2.2) was performed numerically on a computer. The difference of the graphs of Fig. 8 from the corresponding curves of Fig. 7 is entirely due to the presence of the speckle structure in the intensity of the object field. Let us discuss this problem in greater detail.

First we note that the maximum attainable values of the overall efficiency η in both transmission cases—thin and thick-layer—proves to be appreciably lower in holograms of speckle fields: respectively 22% and 64% instead of 34% and 100% for holograms of waves of constant intensity. The decrease in the value of η arises from the strong speckle fluctuations of the local strength of the hologram $\delta M(\mathbf{r}) \sim M$; consequently one can attain values of $M(\mathbf{r})$ close to the optimal only in parts of the area of the hologram.

The value of the pure diffraction efficiency η_0 for small

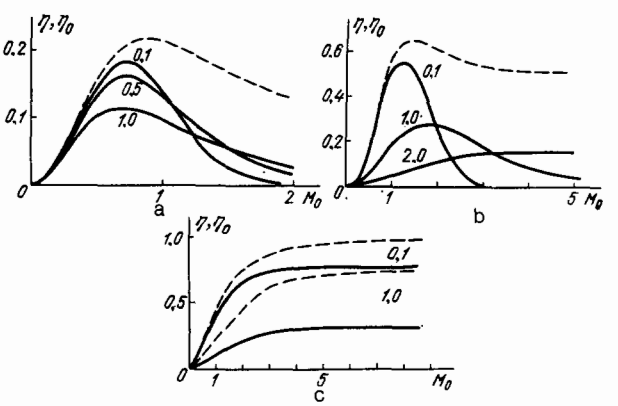

FIG. 8. Dependences of η (dashed lines) and η_0 (solid lines) on M_0 for the different values of I_A/I_B indicated in the diagrams for thin (a), thick-layer transmission (b) and reflection (c) phase holograms having a linear photoresponse.

values of M differs from the overall efficiency η only because of intramodulational distortions (see Sec. 5). When $M > 1$ the relative fraction of the distortions begins to increase sharply. Here also the nonmonotonic dependence of the local efficiency on the strength of the cross-grating comes into play. In regions with $M > M_{\rm opt}$ a larger amplitude $|A(\mathbf{r})|$ in recording corresponds to a smaller reconstructed amplitude $|\tilde{A}(\mathbf{r})|$, i.e., the object field is transmitted with distortions of the amplitude profile. We call these distortions cross-modulational.

For reflection holograms one can remove the intramodulational distortions only when $I_A \ll I_B$. Then when the Bragg condition is exactly fulfilled, i.e., when $X = 0$ and when the strength of the hologram is large enough, $M \gtrsim 1$, the modulus of its local reflection coefficient $\tanh^2 M$ is very close to unity practically throughout the cross section. Here we have $\eta \approx 1$, while the reconstructed field reproduces only the phase but not the amplitude profile of the object field:

$$\tilde{A}(\mathbf{r}) \approx \frac{A(\mathbf{r})}{|A(\mathbf{r})|}\tilde{B}.$$

Remarkably, the reproduction fraction of the exact object field remains amazingly high: averaging over the speckle statistics yields $H = \eta_0/\eta = \pi/4 \approx 79\%$. We can say provisionally that the fundamental information on a speckle field is 80% contained in its phase structure.

Yet if the magnitude of the intraperturbations $\beta_1 I_A$ is of the same order as for the cross-perturbations $\beta_2(I_A I_B)^{1/2}$, then we have $|\delta X| \sim |M|$, and even for large values of the strength of the hologram, the diffraction efficiency η is less than 100%, owing to the impossibility of satisfying the Bragg condition throughout the cross-section of the hologram; simultaneously the reproduction fraction η_0/η also declines.

8.2. Recording with saturation of the photoresponse

Up to now in Sec. 8 we have been treating the situation in which there is no saturation of the local photoresponse: the saturability is $\varphi_0^{-1} \ll 1$. The results obtained show that, for thin and thick-layer holograms of speckle fields, an increase in the diffraction efficiency unavoidably leads to strong distortions of the reconstructed object field. Remarkably, there exist conditions on the saturability φ_0^{-1} (which is a numerical characteristic of the photolayer itself) whose fulfillment may cause the saturation of the photoresponse not only to impair, but conversely, to make the situation for transmission holograms substantially more favorable from the standpoint of diffraction efficiency.[30] Let us discuss this problem in greater detail.

Figure 9 shows the graphs of the dependences of η and η_0 on the parameter proportional to the exposure $M_0 = \varkappa(I_A I_B)^{1/2}$ for different I_A/I_B for a value $\varphi_0^{-1} \approx 0.2$ for thin (Fig. 9a) and $\varphi_0^{-1} \approx 0.1$ for thick-layer phase holograms (Fig. 9b). We can point out the following differences in the behavior of the graphs of Fig. 9a, b as compared with the corresponding graphs of Fig. 8a, b for the case without saturation. First, the values of η and η_0 are somewhat increased for the chosen values of φ_0^{-1}. Second, the dynamic range of exposure values that enable reconstruction with high efficiency and quality proves to be several times larger than when $\varphi_0^{-1} = 0$.

The graphs of Fig. 9a,b were based on the results of numerical calculation. Let us explain the reasons for these qualitative differences. In the presence of saturation the actual strength $M(\mathbf{r})$ of the hologram approaches zero at those sites where the local intensity of the object field $|A(\mathbf{r})|^2$ is small. When $|A(\mathbf{r})|^2 \to \infty$, $M(\mathbf{r})$ also approaches zero, although not too rapidly owing to the effect of saturation. In a

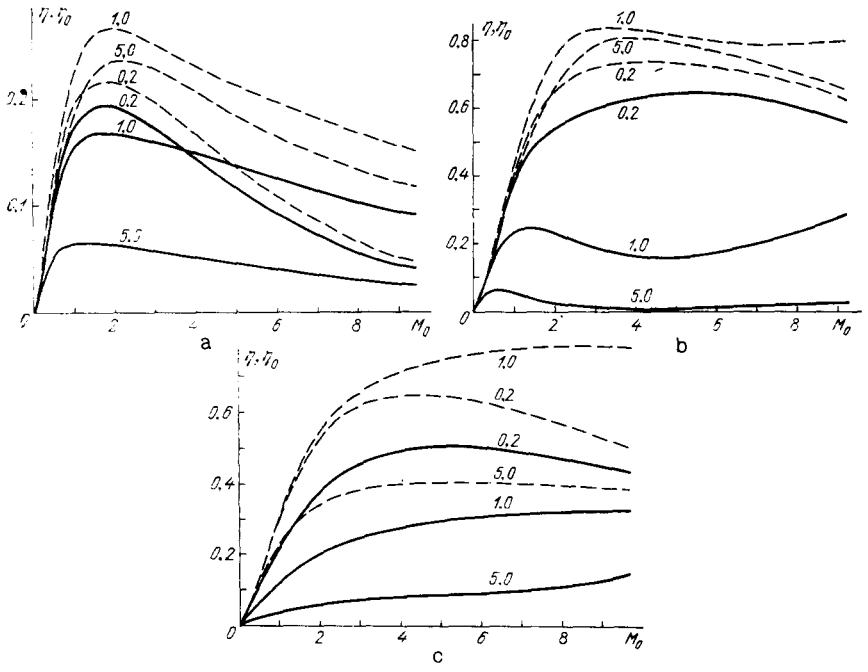

FIG. 9. Dependences of η (dashed lines) and η_0 (solid lines) on M_0 for the different values $I_A/I_B = 0.2$, 1, and 5 for thin ($\varphi_0^{-1} \approx 0.2$) (a), thick-layer transmission ($\varphi_0^{-1} \approx 0.1$) (b) and reflection ($\varphi_0^{-1} = 0.1$) (c) phase holograms recorded with saturation of the photoresponse.

rather broad range of values of the local intensity $|A(\mathbf{r})|^2$ near the maximum of the function $M(|A|)$, the actual strength of the hologram remains almost constant. If this value of M is close to the optimal, $M_{\rm opt} \approx 0.9$ for a thin hologram and $M_{\rm opt} \approx 1.6$ for a thick-layer transmission hologram, while the exposure corresponds to values $M_0 \sim (0.6-1)\varphi_0$, then the local value of η throughout this entire range is close to maximal—34% for thin and 100% for thick layers. Thus an appreciably larger fraction of the area of the hologram operates in an optimal regime under these conditions. As we see from Fig. 5, the maximum value of the actual strength of the hologram corresponds to the optimal value when $\varphi_0^{-1} \approx 0.2$ for thin layers and $\varphi_0^{-1} \approx 0.1$ for thick layers. For larger values of the saturability φ_0^{-1}, the local strength of the hologram does not reach its optimal value over the entire surface. For lower values of φ_0^{-1}, in line with the situation in case of linear recording, the fraction of the area in the hologram of a speckle field corresponding to optimal strength of the hologram decreases.

For reflection holograms large values of M are optimal, $M > 2$. Since saturation can only decrease the strength of a hologram, in the reflection case it only decreases the diffraction efficiency. Thus, for $\varphi_0^{-1} \approx 0.2$, even when $I_A \approx I_B$, the maximum value of the strength of the hologram M does not exceed unity, and the quantity η proves to be $\sim 50\%$ even with an optimal exposure. Figure 9c shows the curves for η and η_0 for a somewhat lower saturability $\varphi_0^{-1} \approx 0.1$ as functions of M_0 for different ratios I_A/I_B of the intensities of the speckle field of the object A and the plane reference wave B during recording.

They show us that also for reflection holograms the presence of speckle structure of the object field appreciably lowers the maximum diffraction efficiency, but now owing to effects of saturation, which are always actually present in a hologram.

For all three forms of holograms in a regime of maximum efficiency, the relative level of distortions of reconstruction $1-(\eta/\eta_0)$ proves to be about the same as for $\varphi_0^{-1} = 0$. In the linear case ($\varphi_0^{-1} = 0$) with the exposure increasing above the optimal, the fraction of distortions $1-(\eta/\eta_0)$ sharply increases. In the case with saturation the situation is the opposite: the rather slow decline in diffraction efficiency when the exposure is increased above the optimal is accompanied by a *decrease* in the relative noise level.

As we see from Fig. 5, in an overexposed hologram ($M_0 \gtrsim \varphi_0$), the given speckle variations $\delta|A|^2/|A|^2$ lead to appreciably smaller intramodulational phase variations that distort the object field.

The most distinct results of experiments designed in goal-directed fashion to study the diffraction efficiency of holograms of speckle fields (holograms of diffuse objects) have been obtained in Ref. 30. The value of the overall efficiency, which we shall denote by the symbol η, is given in Fig. 10 for transmission thick-layer phase holograms as a function of the exposure E_r for different values of I_A/I_B and for two different photomaterials: LOI-2 and dichromated gelatin (DG). The curves correspond to theory and the symbols to experiment. In the layer of DG having rather low saturability, $\varphi_0^{-1} \approx 0.125$, the maximum values of η exceeded 70%. That is, they were appreciably larger than the theoretical limit of 64% pertaining to the case of linear recording.

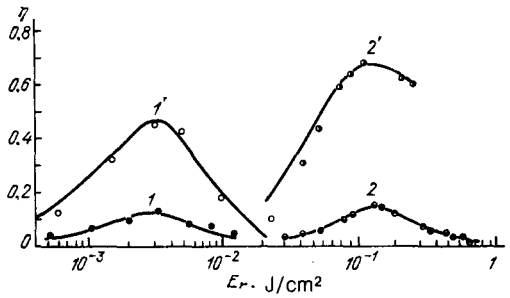

FIG. 10. Dependences[30] of the diffraction efficiency η of holograms of diffuse objects on the exposure E_r for specific layers of LOI-2 (curves *1*, *1'*) and DG (*2*,*2'*) for the different ratios $I_A/I_B = 0.2$ (*1'*), 0.3 (*2'*), and 0.02 (*1*,*2*). Symbols—experimental results.[30]

9. CONCEPT OF THE SPECKLON

Before solving the problem of reconstructing volume holograms of speckle fields, let us study the following model situation. Let a photolayer be exposed solely by the speckle field of the object $A(\mathbf{R})\exp(i\mathbf{k}_A\cdot\mathbf{R})$, so that the dielectric permittivity of the processed medium has the form:

$$\varepsilon(\mathbf{R}) = \varepsilon_0 + \beta_1 |A(\mathbf{R})|^2, \tag{9.1}$$

and the thickness L of the layer is much greater than the length $\lambda/\Delta\theta_A^2$ of a speckle element of the field $A(\mathbf{R})$.

The propagation of the light wave $E(\mathbf{R})$ through a medium having an inhomogeneous $\varepsilon(\mathbf{R})$ given by (9.1) is accompanied by the following two effects.

First, the initial structure of the incident wave is distorted by being scattered by inhomogeneities (i.e., essentially by the intraperturbations $\varepsilon(\mathbf{R}) - \varepsilon_0$). As we shall see below, for weak inhomogeneities these distortions, even when accumulated throughout the thickness of the photolayer, are usually not large. Hence the spatial structure of the field in the photolayer corresponds to propagation as if through a homogeneous medium.

Second, the dielectric permittivity of this effective medium varies as compared with the quantity ε_0. The effective homogeneous permittivity for the field $E(\mathbf{R})$ is determined by the expression[15]

$$\varepsilon_{\rm eff} = \left[\int \varepsilon(\mathbf{R})\,|E(\mathbf{R})|^2 d^3\mathbf{R}\right]\left[\int |E(\mathbf{R})|^2 d^3\mathbf{R}\right]^{-1}. \tag{9.2}$$

That is, it equals the local permittivity $\varepsilon(\mathbf{R})$ averaged over space with a weight determined by the field intensity $|E(\mathbf{R})|^2$.

For almost all fields $E(\mathbf{R})$, including the plane readout wave, the inhomogeneities $\delta\varepsilon(\mathbf{R}) = \beta_1|A(\mathbf{R})|^2$ are uncorrelated with the structure of the field, and then we have

$$\varepsilon_{\rm eff}^{\rm uncorr} = \varepsilon_0 + \beta_1\langle|A|^2\rangle. \tag{9.3}$$

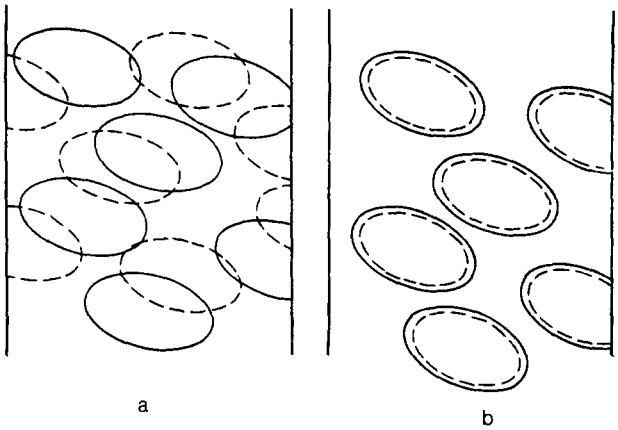

FIG. 11. The speckle field is indicated by dashed contours, the inhomogeneities of the medium by solid contours. Mismatching inhomogeneities (a) yield no spatial resonance, such as is obtained in the case of matched speckle spots (b).

Only for the exceptional case (but precisely a very important one in holography) in which the field $E(\mathbf{R})$ is the object wave itself, $E(\mathbf{R}) \propto A(\mathbf{R})$, is spatial resonance realized between the inhomogeneities of the field and the inhomogeneities of the medium (Fig. 11), and the maxima of the perturbations $\delta\varepsilon(\mathbf{R}) = \beta_1 |A(\mathbf{R})|^2$ coincide with the maxima of the local intensity of the field $E(\mathbf{R})$, so that we have

$$\varepsilon_{\text{eff}}^{(A)} = \varepsilon_0 + \frac{\beta_1 \langle |A|^4 \rangle}{\langle |A|^2 \rangle} = \varepsilon_0 + 2\beta_1 \langle |A|^2 \rangle. \tag{9.4}$$

The second expression of (9.4) is written for the speckle field.

Thus we arrive at an unexpected conclusion: a medium of the form (9.1) has the different effective permittivities (9.3) and (9.4) for the reference wave B and for the speckle field $A(\mathbf{R})$. The approximate solution $E(\mathbf{R}) \approx a(z) A(\mathbf{R}) / \langle |A|^2 \rangle^{1/2}$ of the wave equation (3.1), which describes the propagation of the speckle field in the presence of spatial resonance with the inhomogeneities of the medium has been given a special name—the *specklon*.[15,28,29]

Below we shall have to know the rate of noise buildup in the specklon owing to scattering by the residual fraction of the perturbations of the dielectric permittivity $\delta\varepsilon(\mathbf{R})$ that was not taken into account in defining the effective dielectric permittivity. To do this we must find the extinction coefficient $\mathscr{R}$ (cm^{-1}) characterizing the increase in intensity of the components of $n(\mathbf{r})$ that distort the structure of the original specklon:

$$\frac{d\langle |n|^2 \rangle}{dz} = |a(z)|^2 \mathscr{R}. \tag{9.5}$$

Let us estimate the value of $\mathscr{R}$. At the correlation length $\Delta z_{\text{corr}} \sim \lambda / \Delta\theta_A^2$ of the optical inhomogeneities from (9.1), the relative perturbations of the amplitude of the propagating wave E will amount to $\delta E / E \sim (\omega/c) \Delta z_{\text{corr}} \beta_1 |A|^2$. Therefore the relative intensity of the noise buildup over this length is $(\delta E/E)^2 \sim [\beta_1 |A|^2 / \Delta\theta_A^2]^2$. Since the distortions from different layers separated by the distance Δz_{corr} are uncorrelated, they add in intensity. Consequently, at a distance L containing several lengths of speckle elements, the relative noise level amounts to $[L/\Delta z_{\text{corr}}] \{\beta_1 |A|^2 / \Delta\theta_A]^2$. Upon writing this level in the form $\mathscr{R}L$, we obtain the following estimate for $\mathscr{R}$:

$$\mathscr{R} \sim \frac{(\beta_1 \langle |A|^2 \rangle)^2}{\lambda \Delta\theta_A^2}. \tag{9.6}$$

A more accurate calculation is based on the fact that the term in the induction $\delta D_A(\mathbf{R})$ responsible for the noise buildup of the specklon has the form:

$$\delta D_A(\mathbf{R}) = \beta [|A(\mathbf{R})|^2 - 2\langle |A|^2 \rangle] \frac{a(z) A(\mathbf{R})}{I_A^{1/2}} e^{i\mathbf{k}_A \mathbf{R}}. \tag{9.7}$$

This calculation yields[15,29]

$$\mathscr{R} = \frac{2\pi^2}{\lambda} \left(\frac{\langle \delta\varepsilon \rangle}{\varepsilon} \right)^2 \frac{1}{\Delta\theta_{\text{ef}}^2}, \tag{9.8a}$$

where λ is the wavelength of light in the medium, $\langle \Delta\varepsilon \rangle = \beta_1 I_A$,

$$\frac{1}{\Delta\theta_{\text{ef}}^2} = \iiint d^2\theta_1\, d^2\theta_2\, d^2\theta_3 j_A(\theta_1) j_A(\theta_2) j_A(\theta_3) \delta^{(1)} \times ((\theta_2 - \theta_1)(\theta_2 - \theta_3)), \tag{9.8b}$$

$j_A(\theta)$ is the angular spectrum of the speckle field $A(\mathbf{R})$ normalized to unity, and $(\Delta\theta_A^2)^{\text{eff}}$ is a quantity of the order of the solid angle occupied by the object field. Figure 12 presents the results of experimental measurements of the relative magnitude of the distortions of the specklon I_{noise}/I in a $LiNbO_3$:Fe crystal in a regime of reference-free recording with a local photoresponse. For a fixed exposure the extinction coefficient, as defined by the relationship $I_{\text{noise}}/I = \mathscr{R}L$, proves to be inversely proportional to the square of the angular divergence of the speckle field, in full agreement with theory.

For reference let us give the values of $\Delta\theta_{\text{ef}}^2$ for two concrete forms of angular spectrum of the object field.[15] If $j(\theta) \propto \exp(-\theta^2/\theta_0^2)$, then $\Delta\theta_{\text{ef}}^2 = 2\theta_0^2$; for an angular spectrum of the type of a truncated parabola, $j(\theta) \propto 1 - (\theta^2/\theta_0^2)$, we have $\Delta\theta_{\text{ef}}^2 = 3\pi\theta_0^2/8$.

Since we are interested in applying the specklon theory to holography, we can conveniently express the quantity $\mathscr{R}$ in terms of the strength M and other parameters of the hologram:

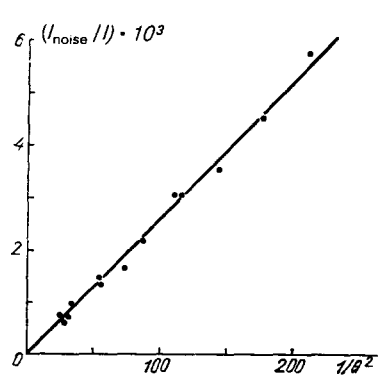

FIG. 12. Dependence of the relative level of extinction distortions of the specklon I_{noise}/I on the inverse square of its angular divergence from an experiment of A. V. Mamaev in the material $LiNbO_3$:Fe.

$$\mathscr{R}L = \cos\theta_A \mid \cos\theta_B \mid M^2 \frac{\beta_1^2 I_A}{\beta_2^2 I_B} \frac{2\lambda}{L\Delta\theta_{\rm ef}^2}. \qquad (9.9)$$

Thus the extinction coefficient $\mathscr{R}$ is proportional to the square of the exposure, $\mathscr{R} \propto M^2$. In a hologram there is usually no reason for making the strength M too large, $M \gtrsim 1.5$, since here the diffraction efficiency is not increased, but the noise level increases.

For the values $\langle\delta\varepsilon\rangle \sim 10^{-4}$, $(\Delta\theta_A)^2 \sim 10^{-2}$ steradian, and $\lambda_{\rm vac} = 0.5\,\mu$m typical of volume holograms, the extinction coefficient is approximately 1.5×10^{-1} cm^{-1}, so that for a typical thickness of the photolayer $L \lesssim 0.1$ cm, the relative level of noise buildup of the specklon is $\mathscr{R}L \sim 1\%$, and the specklon theory proves adequate to problems of volume holography.

The small dimensionless parameter that determines the applicability of the specklon theory[15] is the ratio $\delta\varepsilon_A/\Delta\theta_A^2$, or in another form, the phase advance due to intraperturbations over the length of a speckle element $(\delta\varepsilon_A\omega/c)\Delta z_A$. The three conditions, $I_A/I_B \lesssim 1$, $\Delta z_A \ll L$, and $M \lesssim 1$ that are characteristic of volume holograms ensure the fulfillment of the condition $\delta\varepsilon_A/\Delta\theta_A^2 \ll 1$ with a good margin of safety.

10. RECONSTRUCTION OF SPECKLE FIELDS WITH VOLUME HOLOGRAMS AND THE EFFECT OF SHIFT OF THE SELECTIVITY CURVE

At first glance the electrodynamic problem of reconstructing the speckle field of an object with a volume hologram is extremely complicated. From the mathematical standpoint the problem is to solve the wave equation (3.1), i.e., an equation in partial derivatives, in which the coefficient $\varepsilon(\mathbf{R})$ has a large number of irregular inhomogeneities (intra- and cross-perturbations) that depend substantially on all three spatial coordinates. However, as often happens, in the presence of a small parameter simple physical considerations help in guessing the correct form for seeking the solution.

The scattering of the plane reference wave $\tilde{B}e^{i\mathbf{k}_B\cdot\mathbf{R}}$ in each layer z, $z+dz$ by the cross-grating $\beta_2 A(\mathbf{R})B^* \times\exp[i(\mathbf{k}_A - \mathbf{k}_B)\cdot\mathbf{R}]$ yields a field with the spatial structure $A(\mathbf{R})\exp(i\mathbf{k}_A\cdot\mathbf{R})$ that exactly corresponds to the object field in the given cross section. As we showed in Section 9, this reconstructed field propagates in the medium with the intramodulational perturbations $\beta_1|A(\mathbf{R})|^2$, while practically maintaining its structure.

This implies that the field in the volume of the hologram in the reconstruction process consists of two waves: a plane reference wave and an object specklon coupled by mutual rescattering by the cross-grating:

$$\tilde{E}(\mathbf{R}) = \frac{b(z)}{|\cos\theta_B|^{1/2}} \frac{B}{|B|} \exp(i\mathbf{k}_B\mathbf{R}) + \frac{a(z)}{(\cos\theta_A)^{1/2}} \frac{A(\mathbf{R})}{\langle|A|^2\rangle} \exp[i(\mathbf{k}_B+\mathbf{Q})\mathbf{R}]. \qquad (10.1)$$

All of the further treatment repeats almost verbatim the solution of the problem in Sec. 7.2 of two plane coupled waves. However, in substituting (10.1) into the wave equation (3.1) and deriving the coupled-wave equations for the slow amplitudes $a(z)$ and $b(z)$ we must take account of Eq. (9.2). Consequently the form of the equations for the coupled amplitudes (7.5) is fully conserved. Only the value of the coefficients M and X that enter into them is changed—the strength of the hologram and the Bragg mismatch. The quantity M is now determined by a formula like (3.5), but not in terms of the modulus of the local amplitude, but in terms of the mean value of the intensity, $|A(\mathbf{R})| \to \langle|A|^2\rangle^{1/2} \equiv I_A^{1/2}$. The quantity X acquires an extra term of the form $\delta X = (1/2)\varkappa_1 I_A/\cos\theta_A$.

The shift of the Bragg condition $X = 0$ as compared with that for a hologram of plane waves is caused by the asymmetry that arises between the plane reference wave and the object specklon. In fact, the effective dielectric permittivity for the reference wave, according to (9.3) is $\varepsilon_B^{\rm ef} = \varepsilon_0 + \beta_1(I_A + I_B)$. In contrast, from (9.4) we have for the object specklon $\varepsilon_A^{\rm ef} = \beta_1(2I_A + I_B)$, i.e., doubling of the intramodulational contribution to $\varepsilon_A^{\rm ef}$ owing to spatial resonance. One can say that the Ewald spheres $\mathbf{k}^2 = \omega^2\varepsilon_{\rm ef}/c^2$ for the reference and object waves acquire a small difference of radii, $\mathbf{k}_A| - |\mathbf{k}_B| = (\omega/2c\varepsilon^{-1/2})\beta_1 I_A$.

The condition for efficient reconstruction $X = 0$ in the hologram of a speckle field is attained at a somewhat different frequency and/or direction of readout as compared to a hologram of plane waves recorded in the same geometry and with the same exposure. This property of a volume hologram has been called the effect of shift of the spectral-angular selectivity curve.[29–31] We note that the shift in static phase holograms is not accompanied by a change in the shape of this curve.

The selectivity curves can strongly differ in width for holograms recorded in different media with different geometries; the width in angle and the width in frequency have different dimensionalities. The fact proves to be all the more pleasant that the magnitude of the shift of the selectivity curve owing to the speckle structure of the object field is expressed invariantly in units of the half-width of the curve. In a notation employing the parameter of the Bragg mismatch, the half-width of the curve X (from the zeros in the Born approximation) is $\Delta X(\text{HWOM}) = \pi$. Then the shift of the curve $\delta X_{\rm speckle}$ is

$$\frac{\delta X_{\rm speckle}}{\pi} = \frac{1}{2\pi}\frac{\beta_1}{\beta_2}\left(\frac{I_A\mid\cos\theta_B\mid}{I_B\cos\theta_A}\right)^{1/2} M. \qquad (10.2)$$

In the Born approximation we have $M \approx \eta^{1/2}$, and when $I_A|\cos\theta_B| \approx I_B\cos\theta_A$, $\beta_1 \approx \beta_2$, the relative shift is $\delta X_{\rm speckle}/\pi \approx 0.16\eta^{1/2}$. That is, it amounts to a small fraction of the half-width. When $I_A \ll I_B$ the shift proves to be even smaller.

Figure 13 shows the results of an experiment[32] on transmission phase volume holograms of speckle fields recorded in the material "Reoksan" (see Ref. 33 concerning this material). Angular selective curves were taken[32] for different exposure values. The ratio I_A/I_B was chosen to be large, $I_A/I_B = 15$, in order, first, to increase the relative contribution of the intramodulational perturbations, and second, to avoid the dynamic effects in recording that are inherent in the material "Reoksan." In the experiment the beams $A(\mathbf{R})$ and B were incident symmetrically on the medium, $\theta_A \approx \theta_B = 0.14$ rad (in the medium). Effects of shrinkage and of variation in ε without exposure are absent in "Reok-

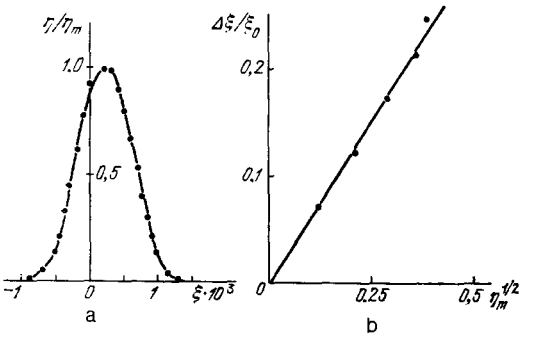

FIG. 13. An experimental study of the selectivity curve of phase holograms in "Reoksan."[32] a—The efficiency η as a function of the angle of deflection ξ from the direction of the reference wave during recording. b—Dependence of the shift $\Delta\xi$ normalized to the half-width ξ_0 of the curve on $\eta_m^{1/2}$.

san." Therefore, in recording the hologram with plane waves with a small exposure at which dynamic effects are absent, the maximum of the angular-selectivity curve corresponds to the direction of the reference wave during recording. We see from Fig. 13a that the direction of optimal readout with an object speckle field differs from the direction of the reference wave during recording. An essential point is that, at the studied values $\eta \lesssim 12\%$, the width of the angular-selectivity curve and its shape practically did not vary, in accord with the theory.

Figure 13b shows the dependence of the magnitude of the shift of the selectivity curve on the parameter $\eta^{1/2}$, which is proportional to the exposure. The straight line corresponding to the theoretical relationship of (10.2) agrees well with the experimental points.

Let us draw the conclusions. Volume holograms of speckle fields are described in terms of diffraction efficiency by practically the same equations as for regular volume holographic gratings. Thus it proves possible to obtain for them a diffraction efficiency close to 100%, in contrast to thin and thick-layer holograms.

Finally let us discuss how this conclusion is affected by the possible saturation of the photomaterial.[30,34] To do this, we should write the induction $\delta D = \delta\varepsilon(\mathbf{R}) \times \widetilde{B} \exp(i\mathbf{k}_B\cdot\mathbf{R})$ that arises upon scattering of the object wave by the perturbations $\delta\varepsilon(\mathbf{R})$ from (6.1) and to project within the framework of the specklon theory $A(\mathbf{R})$ on the field of the specklon, replacing the spatial integration with averaging over the ensemble:

$$M = \frac{kL}{2\varepsilon} \frac{\langle \delta D A^* (\mathbf{R}) \exp[i(\mathbf{k}_B + \mathbf{Q})\mathbf{R}]\rangle}{(I_A I_B)^{1/2}} = M_0 \frac{\exp[-I_B/(I_A + I_H)]}{[1 + (I_A/I_H)]^2} \tag{10.3}$$

Here $M_0 = \varkappa(I_A I_B)^{1/2}$ is the value of the strength of the hologram that would exist in the absence of saturation. We stress that the specklon theory enables us here also to employ the expressions of (7.6) for the diffraction efficiency, provided that we take M from (10.3). We can conveniently compare this dependence of M on the parameters I_A, I_B, and φ_0 with the analogous expression (6.3) for saturable holograms of plane waves by turning to Fig. 5. The presence of the speckle structure, other conditions remaining the same, somewhat lowers the strength of the hologram, owing to the greater level of saturation in the excursions of the speckle field. Therefore the saturability of the photolayer for volume holograms of speckle fields should be very small. For example, one can record a hologram with $\eta \approx 100\%$ at $I_A = I_B/5$ only in a photolayer with a saturability $\varphi_0^{-1} \lesssim 0.09$.

It is convenient to operate at exposure such that $M_0/\varphi_0 = (I_A I_B)^{1/2}/I_{\text{sat}} \lesssim 0.25$, i.e., at not too great a level of local saturation. The reason for this is that the diffraction efficiency increases more slowly than the noise with further increase in the exposure. As we see from the graphs of Fig. 5, in this range of parameters with $I_A \lesssim I_B$, the values of M differ from the strength of the hologram for plane waves by no more than 10%. Moreover, owing to saturation, the intramodulational terms in $\delta\varepsilon(\mathbf{R})$ are recorded more weakly than in a linear medium of the same photosensitivity; consequently *per se* the small shift of the spectral-angular selectivity curve becomes even smaller.

Thus we arrive at an important conclusion: for the values of the parameters of the saturability, exposure, etc., at which a volume hologram gives a high diffraction efficiency, one can reliably calculate the latter by using the results of the theory for holograms of plane waves, both in a linear and in a saturating medium.

11. INTRAMODULATIONAL NOISE OF VOLUME HOLOGRAMS

Another potential advantage of volume holograms in which the length of a speckle element Δz_A is appreciably smaller than the thickness L is the high quality of reconstruction, i.e., the low noise level.

Let us discuss first the cross-modulational noise sources involving the spatial inhomogeneity of the holographic grating. In the Born approximation with a linear response, cross-noise is generally absent (3.3). As the object wave $a_0(z)A(\mathbf{R})$ increases, its inverse scattering by the grating $A^*(\mathbf{R})B\exp[i(\mathbf{k}_B - \mathbf{k}_A)\cdot\mathbf{R}]$ becomes substantial during the reconstruction process. The spatial structure of the polarization of the medium $a(z)|A(\mathbf{R})|^2 B\exp(i\mathbf{k}_B\cdot\mathbf{R})$ contains the homogeneous component $a(z)\langle|A|^2\rangle B\exp \times (i\mathbf{k}_B\cdot\mathbf{R})$, which attenuates the incident plane reference wave owing to efflux of energy into the object field. In addition, in this polarization an inhomogeneous component exists, $(|A(\mathbf{R})|^2 - \langle|A|^2\rangle a(z)B\exp(i\mathbf{k}_B\cdot\mathbf{R})$, which gradually builds up noise in the reference wave. If we assume that $|a(z)|^2 \approx \eta(z/L)^2$, then in the transmission case we can estimate the level of distortions of the reference wave as

$$\langle|b_{\text{noise}}(z)|^2\rangle \approx \frac{1}{3}\eta^2 \frac{\Delta z_A}{L}\left(\frac{z}{L}\right)^3.$$

The reverse scattering of this noise by the grating AB^* in the direction of the object wave leads to relative distortions in it of

$$\frac{\langle|a_{\text{noise}}(L)|^2\rangle}{|a(L)|^2} \approx \frac{1}{12}\eta^2\left(\frac{\Delta z_A}{L}\right)^2. \tag{11.1}$$

For reflection holograms the coefficient 1/12 on the right-hand side of (11.1) is replaced by the coefficient 1/4. If we compare (11.1) with the estimate (5.6) we see that the level of cross-noise in volume holograms amounts to a small frac-

tion $\eta(\beta_2 I_B/12\beta_1 I_A)(\Delta z_A/L)$ of the intramodulational noise. This implies that in a real situation the speckle structure builds up noise in the reconstructed field mainly via the intranoise. Hence, in the present Sec. 11 we shall calculate their level quantitatively to supplement the estimate (5.6).

We shall rewrite the equation for the rate of noise build-up of the object specklon of (9.5) with account taken of a possible slope $\theta_A \neq 0$ in the form

$$\cos\theta_A \frac{d\langle |n|^2\rangle}{dz} = \mathcal{R}|a(z)|^2. \tag{11.2}$$

According to (7.7), for transmission phase holograms we have $|a(z)|^2 = \sin^2(Mz/L)$, and the relative level of distortions of the reconstructed image at the output is

$$\left(\frac{\langle |n|^2\rangle}{|a|^2}\right)_{\text{trans}} = \frac{\mathcal{R}L}{\cos\theta_A}\,\frac{2M-\sin 2M}{4M\sin^2 M}. \tag{11.3}$$

For reflection phase holograms, according to (7.8), we have $|a(z)|^2 = \sinh^2(Mz/L)/\cosh^2 M$, and

$$\left(\frac{\langle |n|^2\rangle}{|a|^2}\right)_{\text{refl}} = \frac{\mathcal{R}L}{\cos\theta_B}\,\frac{\operatorname{sh} 2M-2M}{4M\operatorname{sh}^2 M}. \tag{11.4}$$

In the Born limit, both for transmission and reflection holograms, we have $\eta = |M|^2$, $|a(z)|^2 = \eta z^2/L^2$, and when $\cos\theta_A = \cos\theta_B$, upon using (9.9) we obtain

$$\left(\frac{\langle |n|^2\rangle}{|a|^2}\right)_{\text{Born}} \approx \eta\,\frac{I_A\beta_1^2}{I_B\beta_2^2}\,\frac{\Delta z_A}{L}, \qquad \Delta z_A = \frac{2\lambda}{3\Delta\theta_{\text{cf}}^2}. \tag{11.5}$$

These calculations enabled quantitative expression of the parameter Δz_A from (5.6) in terms of the form of the angular spectrum of the object wave. It is convenient to rewrite Eqs. (11.3) and (11.4) in terms of the noise level in the Born approximation (11.5) with the correction coefficient $\langle|n|^2\rangle/|a|^2 = (\langle|n|^2\rangle/|a|^2)_{\text{Born}} f(M)$, with $f(0) = 1$. Figure 14 presents the variation of the factor $f(M)$ for transmission and reflection holograms. When $M < \pi/2$ the correction does not exceed 50%, so that, even for holograms of high diffraction efficiency, one can calculate the intranoise by the formulas of the Born limit.

Up to now we have been treating the noise in this limit for nonsaturable recording. When we take account of saturation the displacement in the medium that produces the distortion of the object field has the form

$$\delta D_A(\mathbf{R}) = \Big\{[\delta\varepsilon_{\text{in}}(\mathbf{R}) - \langle\delta\varepsilon_{\text{in}}|A|^2\rangle\ I_A^{-1}]\,\frac{a(z)A(\mathbf{R})}{(I_A\cos\theta_A)^{1/2}} + A(\mathbf{R})\left[\frac{\delta\varepsilon_{\text{cr}}(\mathbf{R})}{|A(\mathbf{R})|} - \frac{\langle\delta\varepsilon_{\text{cr}}|A|\rangle}{I_A}\right]\frac{b(z)}{|\cos\theta_B|^{1/2}}\Big\}\,e^{i\mathbf{k}_A\mathbf{R}}. \tag{11.6}$$

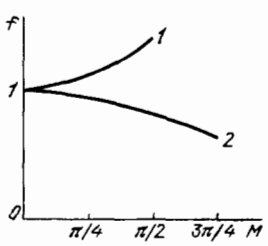

FIG. 14. Dependence of the correction factor f on the strength M of the hologram for transmission (1) and reflection (2) holograms.

Here the quantities $\delta\varepsilon_{\text{in}}(\mathbf{R})$ and $\delta\varepsilon_{\text{cr}}(\mathbf{R})$ are determined by the equations of (6.3). The first term describes the action of the intrainhomogeneities on the propagating field of the object wave, and the second term describes the excitation of noise waves by the cross-grating distorted by saturation. In constructing (11.6) we subtracted the terms that describe spatial resonance of the specklon with the intraperturbations and the coherent rescattering of the reference wave into the specklon by the cross-grating. These terms were already taken into account by Eqs. (9.4) and (10.3). In the absence of saturation ($\beta = \text{const}$, $I_{\text{sat}} \to \infty$), the cross-distortions vanish, and the first term in (11.6) goes over into (9.7). One cannot calculate the noise level using the exact equation (11.6) for an arbitrary level of saturation. However, this is not required, since for volume holograms the only case of any appreciable interest whatever is that in which the cross-grating weakly saturates the photoresponse, $M_0\varphi_0 = |AB|/I_{\text{sat}} \lesssim 1/4$. If we consider precisely this parameter to be small (but not saturation in general) and assume that $I_A \lesssim I_B$, we obtain the following from (11.6):

$$\delta D_A(\mathbf{R}) = e^{i\mathbf{k}_A\mathbf{R}}\,\frac{A(\mathbf{R})}{(I_A\cos\theta_A)^{1/2}} \times [|A(\mathbf{R})|^2 - 2I_A][a(z)\zeta + b(z)\xi], \tag{11.7}$$

$$\zeta = \left(1 - \frac{I_B}{I_{\text{H}}}\right)e^{-I_B/I_{\text{H}}},$$

$$\xi = \frac{(I_A I_B)^{1/2}}{I_{\text{H}}}\left(\frac{I_B}{2I_{\text{H}}} - 1\right)\left(\frac{\cos\theta_A}{|\cos\theta_B|}\right)^{1/2} e^{-I_B/I_{\text{H}}}.$$

Remarkably, in this approximation the spatial structure of the noise from both processes has the same form, namely, the one that occurs in the case of a linear photoresponse. Accordingly one can perform all the calculations by using the extinction coefficient previously derived, i.e., replace in Eq. (11.2) $|a(z)|^2 \to |\zeta a(z) + \xi b(z)|^2$. For exact fulfillment of the Bragg condition $X = 0$, the slow amplitudes $a(z)$ and $b(z)$ are phase-shifted by $\pi/2$, so that the intensity of the noise is determined by the sum of the intensities of the two contributions. Actually the cross-contribution is always small in comparison with the intra-contribution. That is, we can neglect the term $\propto \xi b(z)$. Without taking up the details of integrating (11.2) for transmission and reflection holo-

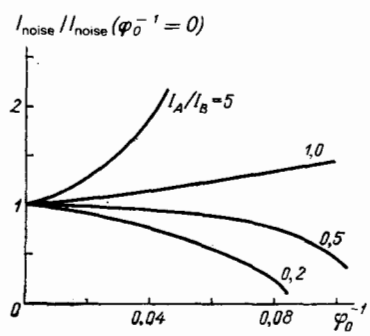

FIG. 15. Level of intramodulational noise of volume holograms normalized to their level in linear recording as a function of the saturability parameter φ_0^{-1} for fixed $M \approx \pi/2$, but various I_A/I_B.

grams, we shall illustrate the results in the graphs of Fig. 15. The intensity of the noise referred to its value in a nonsaturating photolayer is shown for holograms having $M \approx 1.5$ (i.e., with $\eta \approx 1$) as a function of the saturability parameter of the photolayer φ_0^{-1}. These dependences prove to be practically identical for the two types of holograms.

Just as in the cases of thin and thick-layer holograms, there is a remarkable point here. It is psychologically natural to expect that every nonlinearity in transmission leads to additional distortions. However, it turns out that for volume holograms with $I_A \lesssim I_B/2$, a nonlinearity of the local photoresponse in the form of saturation decreases the noise for a given value of η. The reason is that, when $I_A \approx I_B/2$, saturation suppresses the intramodulational inhomogeneities more strongly than the inhomogeneities of the cross-grating.

Let us make another essential remark. The media of large thickness most promising for volume holography, such as "Reoksan" and photorefractive crystals give a dynamic photoresponse $\delta\varepsilon(\mathbf{R})$ directly in the exposure process. As is known,[35,36] the dynamic effects can lead to changes in the relative amplitudes and phases of the recording beams. Moreover, the dynamic processes can cause the weak components obtained by scattering of the reference wave by the initial inhomogeneities of the photolayer to be picked up by the amplification process.[37,38] This pumping implies enhancement of the initial noise during recording.

However, by selecting the angles of inclination and the relationship of intensities of the recording waves A and B, one can reduce to a minimum the variation of their relative amplitudes and phases.[29,32] If the dynamic processes nevertheless persist during recording, then they will mainly result in two effects. The first is a small change in the mean inclination of the fringes of the cross-grating, and the second, a change in the relationship of intensities of the waves throughout the depth of the photolayer. The latter leads to a z-dependence of the amplitudes of the cross-grating and of the intrainhomogeneities. The influence of the first of the effects can be easily compensated by a change in the inclination of the readout wave; then the second effect can be taken into account with good accuracy by substituting into the definition of the strength of the hologram the amplitude of the cross-grating averaged over the depth. Holograms of speckle fields offer appreciable advantages from the standpoint of eliminating the harmful effect of self-amplification of the noise in dynamic recording. Actually the noise adds coherently with the input object speckle field, somewhat altering its concrete realization. However, it is important that this new speckle field is amplified by the reference wave as a unitary whole. That is, the noise level does not increase relative to the object signal.

12. ANTHEM TO VOLUME HOLOGRAMS

It is time to summarize. We have examined in detail the different types of holograms of speckle fields: thin, thick-layer, and volume; transmission and reflection. It is clear at present what their fundamental characteristics and limiting possibilities are. This enables us to compare the different types of holograms with respect to diffraction efficiency and

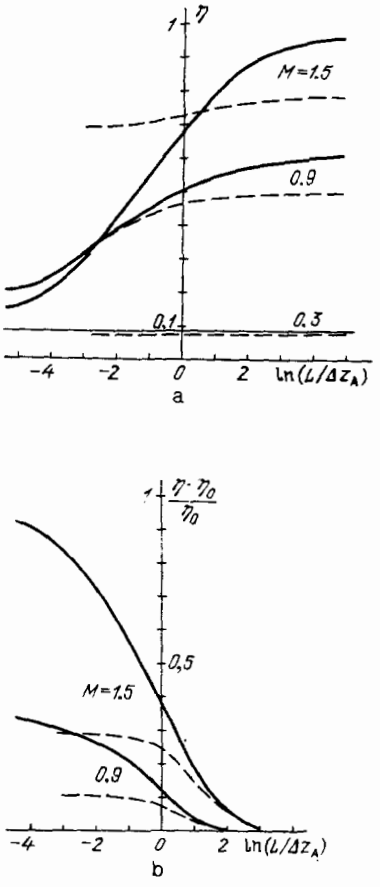

FIG. 16. Dependence of the diffraction efficiency η (a) and of the relative level of distortions (b) on $\ln(L/\Delta z_A)$ for different strengths M for transmission (solid lines) and reflection (dashed lines) holograms.

relative noise level. The comparison turns out, and with a great advantage, in favor of volume holograms. The anthem to volume holograms is the dependences (Fig. 16) of the diffraction efficiency η and the relative noise level $(\eta - \eta_0)/\eta_0$ on the parameter $L/\Delta z_A$ characterizing the degree of "volumeness" of the hologram of the speckle field $A(\mathbf{R})$. Thin holograms correspond to the limit $L/\Delta z_A \ll 1$, thick-layer holograms to $L/\Delta z_A \lesssim 1$, and volume holograms to $L/\Delta z_A \gg 1$.

For the sake of definiteness, the graphs have been drawn for phase holograms with a linear photoresponse. We see from Fig. 15 that only volume holograms allow one to attain maximum diffraction efficiency up to 100%. Their most evident advantage is the rapid decline (as $\Delta z_A/L$) in relative noise level.

The indubitable advantages of volume holograms show how pressing the problem is of creating new recording media of large thickness and perfecting the existing ones, and also of studying them in detail. Apart from this applied conclusion, the authors are no less pleased that it has proved possible to solve such a complex problem of electrodynamics and statistical optics completely, with high accuracy and without simplifying assumptions.

13. BIBLIOGRAPHICAL NOTES

The addition of a large number of monochromatic waves with independent phases was treated by Rayleigh (see, e.g., Refs. 21 and 39). Apparently the first observations of the speckle structure of a light field were made in Ref. 40 and then with especial clarity and with a theoretical analysis by Max von Laue.[41] Professor I. A. Yakovlev has kindly called our attention to Refs. 40 and 41. After the invention of lasers speckle fields began to appear everywhere. In addition to the general monographs of Refs. 13, 14, 42, 43 we note here a number of studies on the structure of speckle fields,[44,48] their application in interferometry,[45,46] and on dislocations of the wave front of speckle fields.[47] Holograms using coded (i.e., speckle-inhomogeneous) reference waves and the so-called "reference-free" holograms have been studied in a number of paper; we note here Refs. 48 and 49.

Thin phase holograms of speckle fields have been treated in Refs. 50–52. Holograms in which the higher diffraction orders are not excited have usually been called volume holograms to distinguish them from thin holograms. The classification used in this review, which distinguishes: 1) volume holograms proper, 2) thick-layer holograms, and 3) thin holograms of speckle fields, was introduced by the authors.[53] The diffraction efficiency of thick-layer phase holograms of speckle fields has been studied theoretically and experimentally in Refs. 30, 53, and 54.

Calculations have been performed[27] of the diffraction efficiency and noise of holograms of speckle fields of all types. The effect of saturation of the photoprocess on the overall diffraction efficiency has been studied experimentally and discussed theoretically in Ref. 30. The theory of saturation effects, including the calculation of the noise, for thin and thick-layer transmission and reflection holograms presented in this review is that of the authors. The selective properties of thick-layer and volume holograms have become the object of intensive studies since the ground-laying study of Yu. N. Denisyuk.[10] We follow our study[26] in presenting the problem of selectivity in Sec. 4.

The theory of coupled waves was first applied to holography by H. Kogelnik.[12] A detailed presentation of the results of this theory, including gratings of sinusoidal profile with smooth inhomogeneity, is found in the monograph of Ref. 74. One of the first attempts to transfer the theory of coupled waves to the case of volume holograms of speckle fields was made in Ref. 55. An important stimulating role was played by the study of V. G. Sidorovich,[56] in which the diffraction efficiency of a paraxial transmission phase volume hologram was first calculated, with account taken of the intramodulational contributions to the phase velocity of the speckle wave.

Here an expansion was used of the speckle field of the object wave into discrete angular components, together with the concept of "modes of a hologram." It was followed by a number of studies[26,57–66] that employed the methods of mode theory of volume holograms initiated by V. G. Sidorovich and devoted to different aspects of the reconstruction process. A space-frequency variant of the theory of three-dimensional holograms was developed in Refs. 67–70 that differs from the mode theory by expansion in a continuous spectrum of angular components.

In this review for constructing a theory of volume holograms we have employed the concept of a "*specklon*" introduced in Ref. 28, which characterizes a speckle field with altered phase velocity and a certain extinction. Thereby one can obtain the needed results by a most simple and pictorial method. This approach has been developed in Refs. 15, 26, 29, 31, and 71. A language close to it has been used in Ref. 72. The shift of the selectivity curve of a static volume hologram was discovered experimentally in Ref. 32. The saturation of the photoresponse of volume holograms was treated in Refs. 34 and 73 as applied to calculating the diffraction efficiency. The calculation of the intramodulational noise of volume holograms of speckle fields is due to the authors of this review; it was published for an unsaturated photoresponse in Refs. 29 and 58.

Dynamic effects are very important in recording holograms of great thickness in materials such as "Reoksan" and photorefractive crystals. In this review, which is devoted to static holography, these problems have hardly been discussed. These problems for holograms of speckle fields have been studied in Refs. 29, 67, 70, and 75.

The authors are deeply obliged to Yu. N. Denisyuk and G. V. Skrotskiĭ for attention and interest in this study, and to N. G. Vlasov, A. V. Mamaev, Yu. I. Ostrovskiĭ, V. G. Sidorovich, and M. S. Soskin for valuable discussions.

[1)]The senior author of this review (B. Z.) had the good fortune of associating with R. V. Khokhlov in the heroic period 1962–1966 when Rem Viktorovich and S. A. Akhmanov were beginning in the Physics Department of the M. V. Lomonosov State University in Moscow in the chairs of Professor V. V. Migulin and Professor S. D. Gvozdover to become involved in nonlinear optics. The aforementioned author considers himself a student of this remarkable school of nonlinear and coherent optics, "perhaps not the most diligent and not the most obedient." It is difficult to convey in words the radiation of human kindness and interest and high scientific demands that stemmed from Rem Viktorovich. It is a great pity that Rem Viktorovich did not have time to carry out all that was within his powers, that was intended and destined for him in world and Soviet science. And at the same time one is glad to see how his scientific "family" is living and developing, and how his "scientific" children and grandchildren are growing. To no lesser degree we apply these words also to Elena Mikhaĭlovna, to their children and grandchildren, to the remarkable family of Rem Viktorovich in the "ordinary" sense.

[2)]Sometimes one uses the word "intermodulational," borrowed from radiotechnology.

[3)]However, there is an example of the so-called photorefractive crystals,[16,17] for which the reverse relationship can also exist.

[4)]We call the reader's attention to the importance of the choice of criterion for the width of the curve. Thus, for the same curve $\sin^2 X/X^2$ the half-width at an intensity half the maximum (Half-Width–Half-Maximum) is $\Delta X(\mathrm{HWHM}) \approx 1.4$, i.e., about 4.5 times smaller than the quantity $\Delta X(\mathrm{FWOM})$.

[1]R. J. Collier, C. B. Burckhardt, and L. H. Lin, Optical Holography, Academic Press, New York, 1971 [Russ. transl., Mir, M., 1973].
[2]G. W. Stroke, An Introduction to Coherent Optics and Holography, Academic Press, New York, 1966 [Russ. transl., Mir, M., 1967].
[3]L. M. Soroko, Osnovy golografii i kogerentnoĭ optiki, Nauka, M., 1971 [Engl. transl., Holography and Coherent Optics, Plenum Press, New York, 1980].

[4]J. W. Goodman, Introduction to Fourier Optics, McGraw-Hill, New York, 1968 [Russ. transl., Mir, M., 1970].
[5]Yu. I. Ostrovskiĭ, Golografiya i ee primenenie (Holography and Its Applications), Nauka, L., 1973.
[6]Handbook of Optical Holography, ed. H. J. Caulfield, Academic Press, N. Y. 1979 [Russ. transl., Mir, M., 1982].
[7]J. D. Gabor, Nature **161**, 777 (1948).
[8]W. L. Bragg, Nature **166**, 399 (1950).
[9]E. N. Leith and J. Upatnieks, J. Opt. Soc. Am. **53**, 1377 (1963).
[10]Yu. N. Denisyuk, Opt. Spektrosk. **15**, 522 (1963) [Opt. Spectrosc. (USSR) **15**, 279 (1963)].
[11]H. Kogelnik, Bell Syst. Tech. J. **48**, 1835 (1969).
[12]H. Kogelnik, *ibid.*, p. 2909.
[13]J. C. Dainty, ed., Laser Speckle and Related Phenomena, Springer-Verlag, Berlin, 1975.
[14]M. Franson, Optika speklov (Speckle Optics), Mir., M., 1980.
[15]B. Ya. Zel'dovich, N. F. Pilipetskiĭ, and V. V. Shkunov, Obrashchenie volnovogo fronta (Wave Front Reversal), Nauka, M., 1985.
[16]V. L. Vinetskiĭ, N. V. Kukhtarev, S. G. Odulov, and M. S. Soskin, Usp. Fiz. Nauk **129**, 113 (1979) [Sov. Phys. Usp. **22**, 742 (1979)].
[17]P. Günter, Phys. Rep. **93**, 199 (1982).
[18]M. Born and E. Wolf, Principles of Optics, 4th ed., Pergamon Press, Oxford (1970) [Russ. transl., Nauka, M., 1973].
[19]L. D. Landau and E. M. Lifshitz, Teoriya polya, Nauka, M., 1973 [Engl. transl., The Classical Theory of Fields, 4th ed., Pergamon Press, Oxford, 1975].
[20]W. B. Davenport, Jr. and W. L. Root, Introduction to Random Signals and Noise, McGraw-Hill (1958) [Russ. transl., IL, M., 1960].
[21]S. M. Rytov, Vvedenie v statisticheskuyu radiofiziku. Ch. 1: Sluchaĭnye protsessy (Introduction to Statistical Radiophysics. Part 1: Random Processes), Nauka, M., 1976.
[22]S. A. Akhmanov, Yu. E. D'yakov, and A. S. Chirkin, Vvedenie v statisticheskuyu radiofiziku i optiku (Introduction to Statistical Radiophysics and Optics), Nauka, M., 1981.
[23]S. A. Akhmanov and R. V. Khokhlov, Problemy nelineĭnoi optiki, VINITI, M., 1964 (Engl. transl., Nonlinear Optics, Gordon and Breach, New York, 1972).
[24]A. V. Mamaev, Yu. V. Mukhin, N. F. Pilipetskiĭ, and V. V. Shkunov, Kvantovaya Elektron. (Moscow) **10**, 1483 (1983) [Sov. J. Quantum Electron. **13**, 967 (1983)]; A. V. Mamaev, N. F. Pilipetskiĭ, and V. V. Shkunov, *ibid.* **11**, 1275 (1984) [Sov. J. Quantum Electron. **14**, 862 (1984)].
[25]B. Ya. Zel'dovich and V. V. Shkunov, *ibid.* **4**, 1090 (1977) [Sov. J. Quantum Electron. **7**, 610 (1977)].
[26]B. Ya. Zel'dovich, V. V. Shkunov, and T. V. Yakovleva, Modovaya teoriya ob"emnykh gologramm (Mode Theory of Volume Holograms), Preprint of the P. N. Lebedev Physics Institute, Academy of Sciences of the USSR, Moscow, No. 54, Moscow, 1979.
[27]B. Ya. Zel'dovich, A. V. Mamaev, A. Yu. Khaĭkin, V. V. Shkunov, and T. V. Yakovleva, Fizicheskie osnovy i prikladnye voprosy golografii (Physical Bases and Applied Problems of Holography), B. P. Konstantinov Leningrad Institute of Nuclear Physics, Academy of Sciences of the USSR, Gatchina, L., 1985, p. 210.
[28]B. Ya. Zel'dovich, N. F. Pilipetskiĭ, and V. V. Shkunov, Usp. Fiz. Nauk **138**, 249 (1982) [Sov. Phys. Usp. **25**, 713 (1982)].
[29]B. Ya. Zel'dovich and V. V. Shkunov, Izv. Akad. Nauk SSSR Ser. Fiz. **48**, 1545 (1984) [Bull. Acad. Sci. USSR, Phys. Ser. **48**(8), 85 (1984)].
[30]A. L. Churaev, D. I. Stasel'ko, and A. A. Benken, Zh. Tekh. Fiz. **54**, 306 (1984) [Sov. Phys. Tech. Phys. **29**, 178 (1984)].
[31]B. Ya. Zel'dovich and V. V. Shkunov, Kvantovaya Elektron. (Moscow) **11**, 2162 (1984) [Sov. J. Quantum Electron. **14**, 1443 (1984)].
[32]E. A. Sander, V. V. Shkunov, and S. A. Shoĭdin, Zh. Eksp. Teor. Fiz. **88**, 116 (1985) [Sov. Phys. JETP **61**, 68 (1985)].
[33]G. I. Lashkov and V. I. Sukhanov, Opt. Spektrosk. **47**, 1126 (1979) [Opt. Spectrosc. (USSR) **47**, 625 (1979)].
[34]B. Ya. Zel'dovich and T. V. Yakovleva, Kvantovaya Elektron. (Moscow) **7**, 519 (1980) [Sov. J. Quantum Electron. **10**, 295 (1980)].
[35]V. L. Vinetskiĭ, N. V. Kukhtarev, V. B. Markov, S. G. Odulov, and M. S. Soskin, Izv. Akad. Nauk SSSR Ser. Fiz. **41**, 811 (1977). [Bull. Acad. Sci. USSR, Phys. Ser. **41**(4), 135 (1977)].
[36]V. I. Belinicher and B. I. Sturman, Usp.Fiz. Nauk **130**, 415 (1980) [Sov. Phys. Usp. **23**, 199 (1980)].
[37]R. Magnusson and T. K. Gaylord, Appl. Opt. **13**, 1545 (1974).
[38]V. V. Obukhovskiĭ and A. V. Stoyanov, Kvantovaya Elektron. (Moscow) **12**, 563 (1985) [Sov. J. Quantum Electron. **15**, 367 (1985)].
[39]J. W. S. Rayleigh, The Theory of Sound, 2nd ed., Macmillan, London, 1986 [Russ. transl., Gostekhizdat, M., 1955, Vol. 1].
[40]K. Exner, Wiener Ber. **76**, 522 (1877).
[41]M. von Laue, Verh. Deutsch. Phys. Ges., 1144 (1915).
[42]I. S. Klimenko, Golografiya sfokusirovannykh izobrazheniĭ i spekl-interferometriya (Holography of Focused Images and Speckle Interferometry), Nauka, M., 1985.
[43]Yu. I. Ostrovskiĭ, M. M. Butusov, and G. V. Ostrovskaya, Golograficheskaya interferometriya (Holographic Interferometry), Nauka, M., 1977 [Engl. transl., Interferometry by Holography (Springer series in optical science: V. 20), Springer-Verlag, Heidelberg–N. Y., 1980].
[44]S. I. Kozel and G. R. Lokshin, Opt. Spektrosk. **33**, 165 (1972) [Opt. Spectrosc. (USSR) **33**, 89 (1972)].
[45]N. G. Vlasov and Yu. P. Presnyakov, Opticheskaya golografiya (Optical Holography), LDNTP, L., 1972, p. 51.
[46]N. G. Vlasov, Yu. P. Presnyakov, and E. G. Semenov, Opt. Spektrosk. **37**, 369 (1974) [Opt. Spectrosc. (USSR) **37**, 210 (1974)].
[47]N. B. Baranova and B. Ya. Zel'dovich, Zh. Eksp. Teor. Fiz. **80**, 1789 (1980) [Sov. Phys. JETP **53**, 925 (1980)]; N. B. Baranova, B. Ya. Zel'dovich, A. V. Mamaev, N. F. Pilipetskiĭ, and V. V. Shkunov, *ibid.* **83**, 1702 (1982) [Sov. Phys. JETP **56**, 983 (1982)]; N. B. Baranova, A. V. Mamaev, N. F. Pilipetsky, V. V. Shkunov, and B. Ya. Zel'dovich, J. Opt. Soc. Am. **73**, 525 (1983).
[48]V. K. Polyanskiĭ and L. V. Koval'skiĭ, Opt. Spektrosk. **35**, 345 (1973) [Opt. Spectrosc. (USSR) **35**, 200 (1973)]; V. K. Polyanskiĭ and V. P. Polyanskiĭ, Fundamental'nye osnovy opticheskoĭ pamyati i sredy (Fundamental Bases of Optical Memory and Media), Vishcha shkola, Kiev, 1985, p. 22; V. K. Polyanskiĭ, S. N. Roslyanov, and V. V. Tarnovetskiĭ, Ukr. Fiz. Zh. **25**, 645 (1980).
[49]E. A. Sander, V. I. Sukhanov, and S. A. Shoĭdin, Opticheskaya golografiya (Optical Holography), Nauka, L., 1983, p. 77.
[50]C. H. F. Velzel, Opt. Commun. **3**, 133 (1971); Optica Acta **20**, 585 (1973).
[51]V. I. Lokshin and G. B. Semenov, Materialy IV Vsesoyuznoĭ shkoly po golografii (Materials of the 4th All-Union School on Holography), LFTI AN SSSR, L., 1973, p. 313.
[52]B. Ya. Zel'dovich and P. B. Lerner, Kvantovaya Elektron. (Moscow) **8**, 1886 (1981) [Sov. J. Quantum Electron. **11**, 1141 (1981)].
[53]B. Ya. Zel'dovich, V. V. Shkunov, and T. V. Yakovleva, *ibid.* **10**, 1581 (1983) [Sov. J. Quantum Electron. **13**, 1040 (1983)].
[54]C. Leonard and J. Upatniecks, J. Opt. Soc. Am. **60**, 297 (1971).
[55]V. V. Aristov and V. Sh. Shekhtman, Usp. Fiz. Nauk **104**, 51 (1971) [Sov. Phys. Usp. **14**, 263 (1971)].
[56]V. G. Sidorovich, Zh. Tekh. Fiz. **46**, 1306 (1976) [Sov. Phys. Tech. Phys. **21**, 742 (1976)].
[57]A. A. Leshchev and V. G. Sidorovich, Opt. Spektrosk. **44**, 302 (1978) [Opt. Spectrosc. (USSR) **44**, 175 (1978)].
[58]B. Ya. Zel'dovich, V. V. Shkunov, and T. V. Yakovleva, Preprint of the P. N. Lebedev Physics Institute, Academy of Sciences of the USSR, No. 26, Moscow, 1979.
[59]V. G. Sidorovich and V. V. Shkunov, Opt. Spektrosk. **44**, 1001 (1978) [Opt. Spectrosc. (USSR) **44**, 586 (1978)].
[60]B. Ya. Zel'dovich and V. V. Shkunov. a) Preprint of the P. N. Lebedev Physics Institute of the Academy of Sciences of the USSR, No. 57, Moscow, 1978; b) Fizicheskie osnovy golografii (Physical Bases of Holography) (Materials of the 10th All-Union School on Holography), B. P. Konstantinov Leningrad Institute of Nuclear Physics, Academy of Sciences of the USSR, Gatchina, L., 1978, p. 46; c) Appl. Opt. **18**, 3633 (1979).
[61]B. Ya. Zel'dovich and V. V. Shkunov, Preprint of the P. N. Lebedev Physics Institute, Academy of Sciences of the USSR, No. 266, Moscow, 1978.
[62]B. Ya. Zel'dovich and V. V. Shkunov, Kvantovaya Elektron. (Moscow) **6**, 1533 (1979) [Sov. J. Quantum Electron. **9**, 897 (1979)].
[63]V. G. Sidorovich, see Ref. 60b, p. 161.
[64]N. B. Baranova, B. Ya. Zel'dovich, V. V. Shkunov, and T. V. Yakovleva, Materials of the 12th All-Union School on Holography, B. P. Konstantinov Leningrad Institute of Nuclear Physics, Academy of Sciences of the USSR, Gatchina, L., 1980, p. 3.
[65]A. A. Leshchev and V. G. Sidorovich, in: Opticheskaya golografiya (Optical Holography), ed. Yu. N. Denisyuk, Nauka, L., 1979, p. 42.
[66]B. Ya. Zel'dovich, V. V. Shkunov, and T. V. Yakovleva, in: Problemy opticheskoĭ golografii (Problems of Optical Holography), ed. Yu. N. Denisyuk, Nauka, L., 1981, p. 80.
[67]V. I. Sukhanov and Yu. L. Korzinin, Pis'ma Zh. Tekh. Fiz. **8**, 1144 (1982) [Sov. Tech. Phys. Lett. **8**, 491 (1982)].
[68]Yu. L. Korzinin and V. I. Sukhanov, *ibid.* **9**, 1254 (1983) [Sov. Tech. Phys. Lett. **9**, 538 (1983)].
[69]Yu. L. Korzinin and V. I. Sukhanov, Opt. Spectrosk. **56**, 763 (1984)

[Opt. Spectrosc. (USSR) **56**, 467 (1984)].
[70]Yu. L. Korzinin and V. I. Sukhanov, Pis'ma Zh. Tekh. Fiz. **10**, 1073 (1984) [Sov. Tech. Phys. Lett. **10**, 454 (1984)].
[71]B. Ya. Zel'dovich and V. V. Shkunov, Fizicheskie osnovy golografii (Physical Bases of Holography): Proceedings of the 15th School on Holography, LFTI AN SSSR, L., 1983, p. 104.
[72]A. E. Krasnov, Kvantovaya Elektron. (Moscow) 7, 818 (1980) [Sov. J. Quantum Electron. **10**, 466 (1980)].
[73]E. A. Sander and S. A. Shoidĭn, Sbornik trudov IV vsesoyuznoĭ konferentsii po golografii (Collection of Papers of the 4th All-Union Conference on Holography), VNIIRI, Erevan, 1982, p. 172.
[74]L. Solymar and D. J. Cooke, Volume Holography and Volume Gratings, Academic Press, New York, 1981.
[75]A. M. Dukhovnyĭ and D. I. Stasel'ko, Pis'ma Zh. Tekh. Fiz. **8**, 1009 (1982) [Sov. Tech. Phys. Lett. **8**, 436 (1982)].
[76]N. Bloembergen (Ed.), Nonlinear Spectroscopy, North Holland, Amsterdam, 1977 [Russ. transl., Mir, M., 1979, p. 24].
[77]R. V. Khokhlov, Radiotekh. Elektron. **6**, 917 (1961) [Radio Eng. Electron. Phys. (USSR) **6**(6), 77 (1961)].
[78]R. V. Khokhlov., *ibid.*, p. 1116 [Radio Eng. Electron. Phys. (USSR) **6**(7), 128 (1961)].
[79]D. I. Stasel'ko and A. L. Churaev, Zh. Tekh. Fiz. **56**, 324 (1986) [Sov. Phys. Tekh. Phys. **31**, 197 (1986)].
[80]D. I. Stasel'ko and V. S. Obraztsov, Zh. Nauchn. Prikl. Fotogr. Kinematogr. **17**, 115 (1972).
[81]D. I. Stasel'ko and A. L. Churaev, Opt. Spektrosk. **57**, 677 (1984) [Opt. Spectrosc. (USSR) **57**, 411 (1984)].

Translated by M. V. King